Charm and J/ψ cross-section measurements at 13 TeV with real-time calibration

Patrick Spradlin
on behalf of the LHCb collaboration

University of Glasgow Particle Physics

LHC Seminar
07 October 2015
CERN, Geneva, Switzerland

Outline

LHCb at P8


LHCb

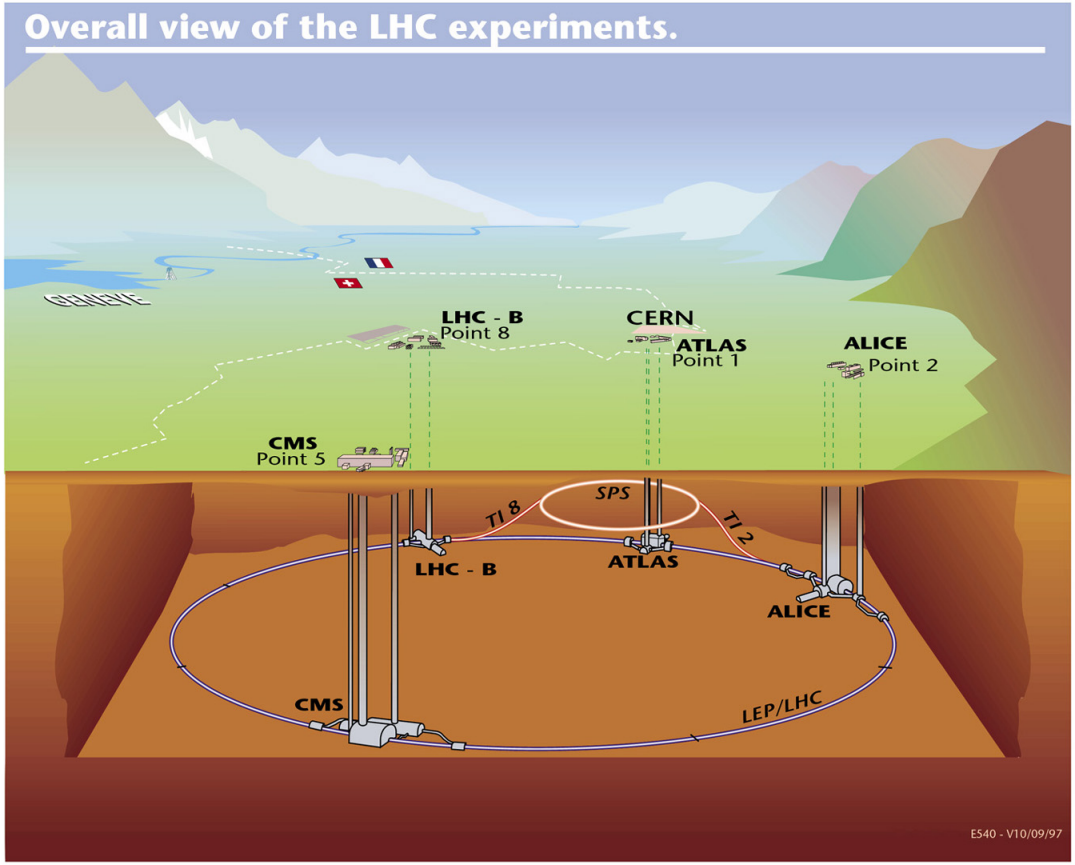
Overall view of the LHC experiments.
LHC - B
Point 8
CERN
ATLAS
Point 1
ALICE
Point 2
CMS
Point 5
SPS
TI 8
TI 2
LHC - B
ATLAS
ALICE
CMS
LEP/LHC
E540 - V10/09/97

LHCb

LHCb: a single-arm forward spectrometer at the LHC.

Optimized for heavy flavor physics in *pp* collisions.

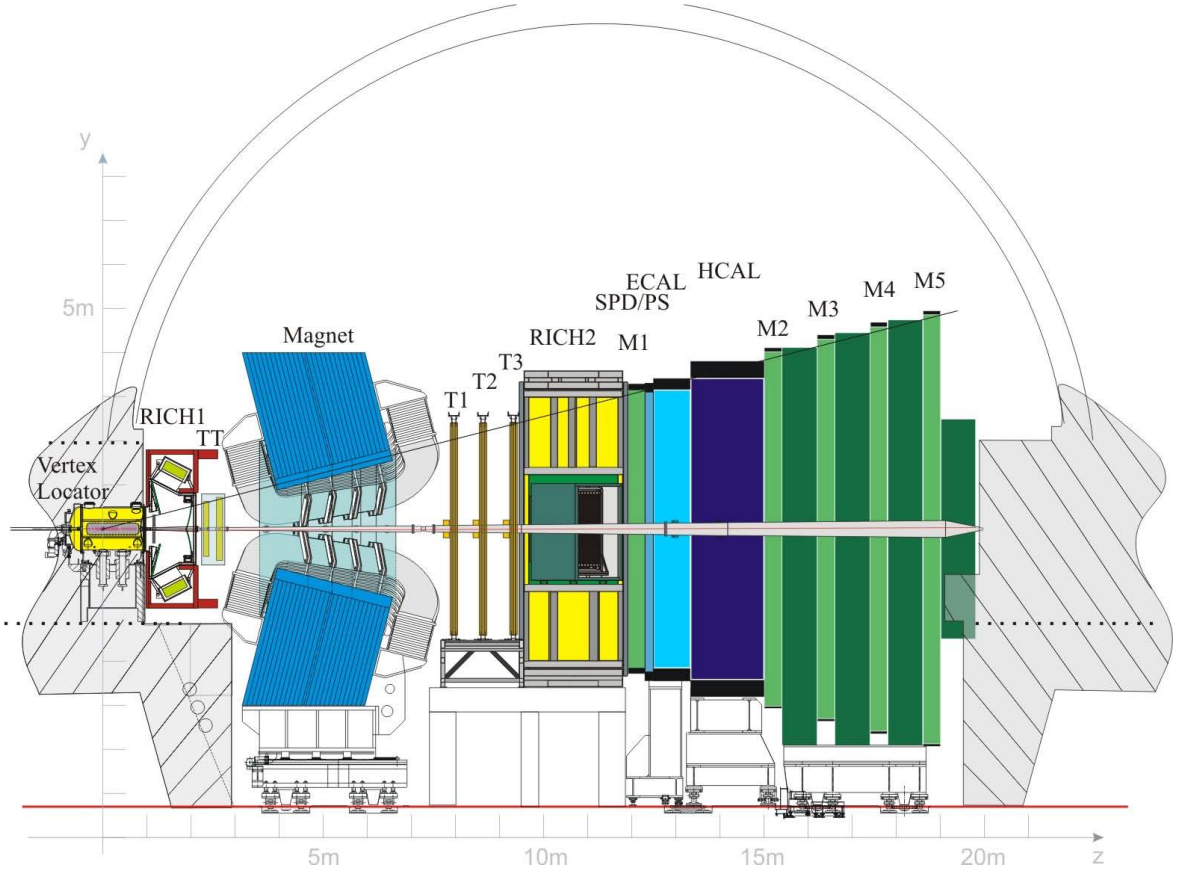

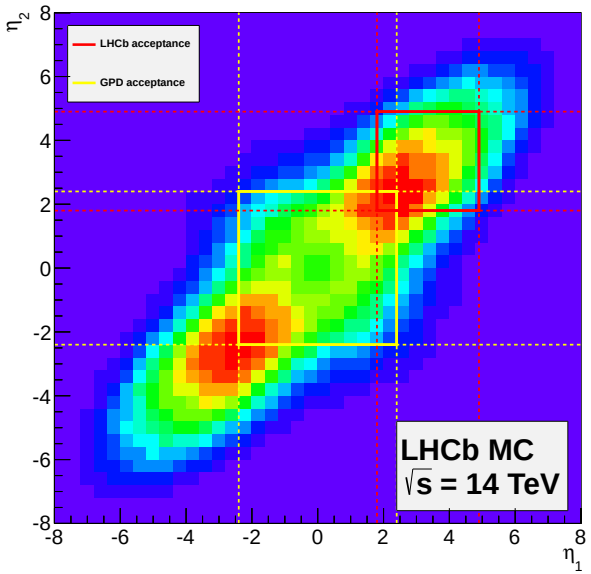

Pseudorapidity range unique among the LHC detectors.

Complementary to ATLAS and CMS.

LHCb detector

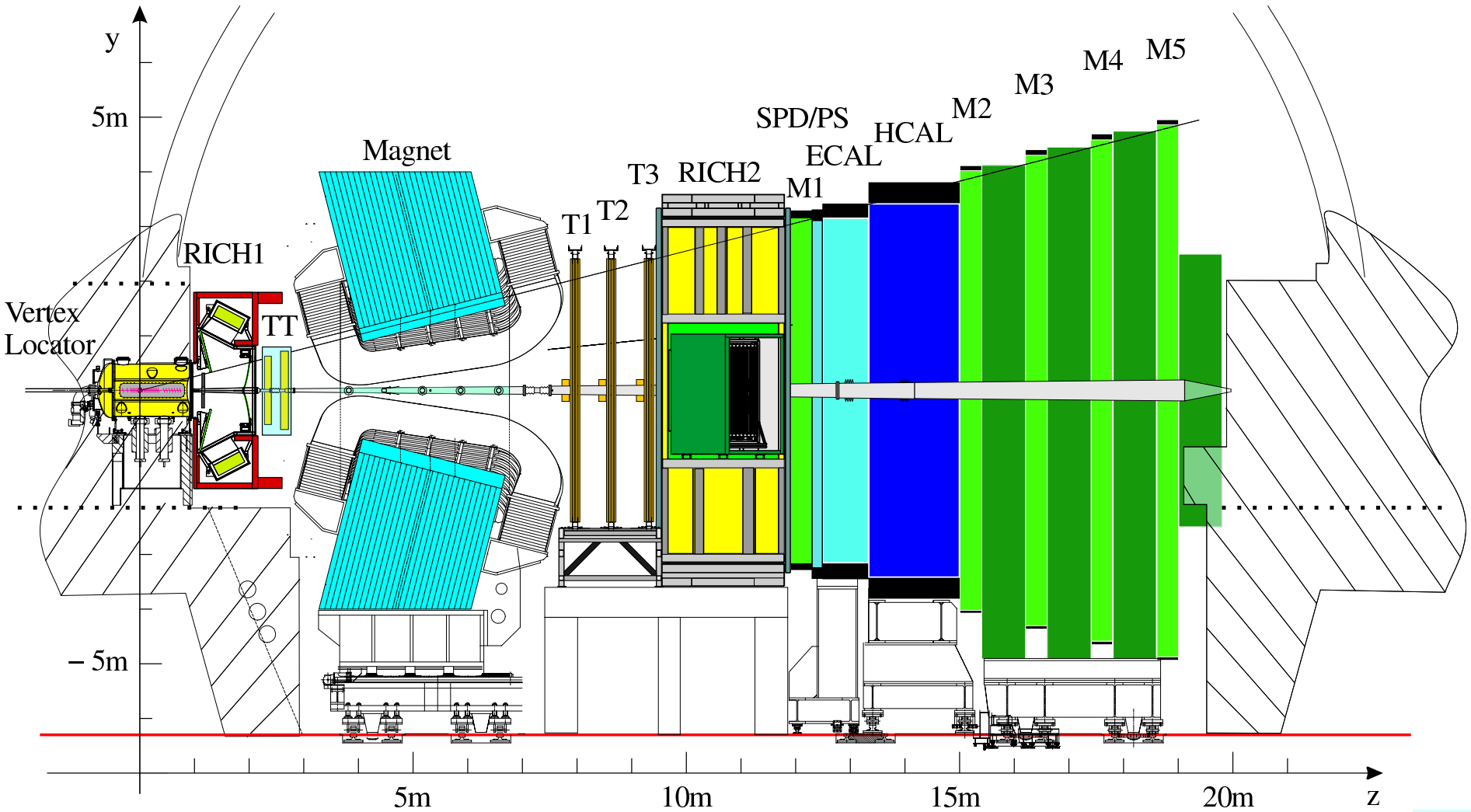

Early 2015 Measurements Task Force

LHC's $\sqrt{s} = 13\,\text{TeV}$ operation opens a new regime for production measurements!

LHCb created the Early 2015 Measurements Task Force to coordinate analysis and calibration activities to ensure the rapid exploitation of the LHCb data to be taken in 2015, specifically for production measurements at the new collision energy.

The task force coordinates most aspects of the operational and analysis planning for the data collected at $\sqrt{s} = 13\,\text{TeV}$,

- Collision conditions,
- Special triggers,
- Data processing,
- Luminosity calibration,
- Measurements of PID and tracking efficiency,

Physics measurements!

DATA COLLECTION

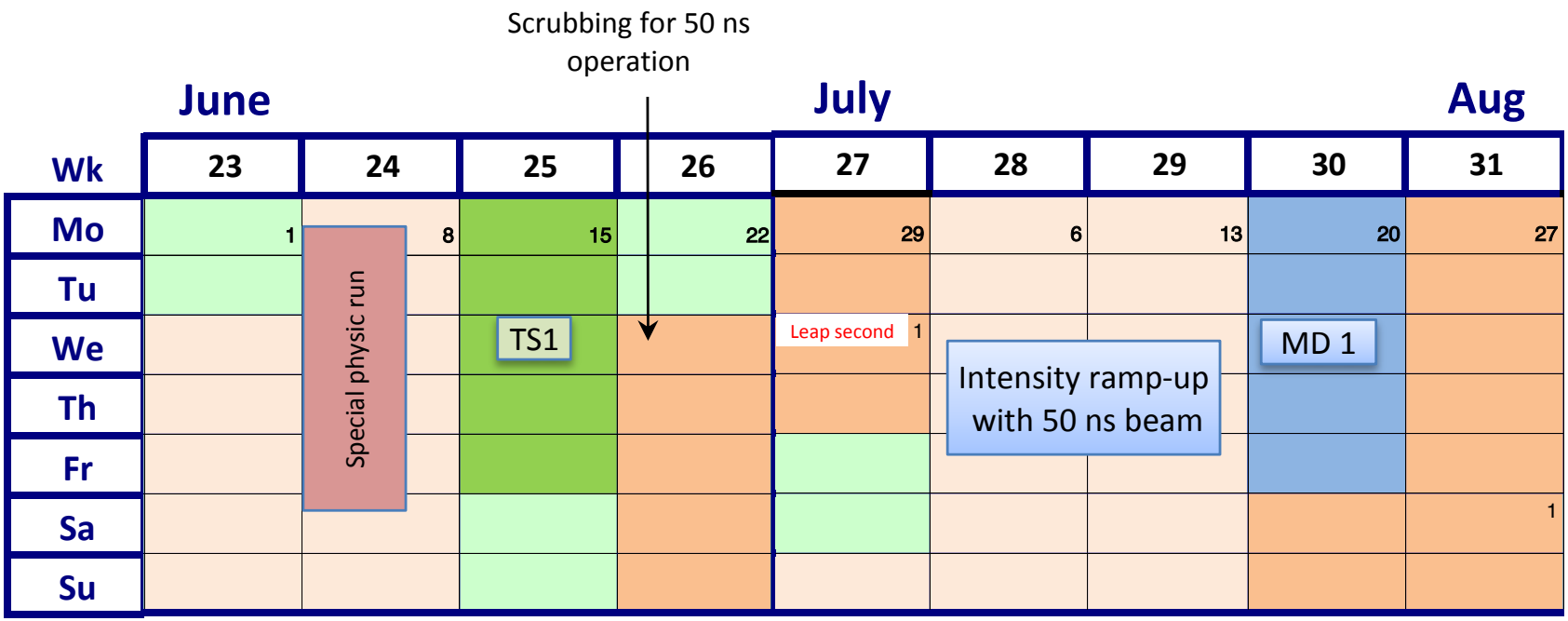

The July 50 ns intensity ramp was used for primary data collection

- Calibration and full system validation with the June first collisions,
- Luminosity calibration with Beam Gas imaging also in June,
- Smaller collision rate $\Rightarrow$ low-p_{T} triggers,
- Luminosity leveling $\Rightarrow$ consistent collision conditions.

DATA COLLECTION

Dedicated data set to support a broad program of production measurements

- Soft QCD and strangeness production,
  - Forward energy flow,
  - Charged particle multiplicity,
  - Total inelastic cross-section,
  - K^0_S production cross-section,
  - ϕ production cross-section,
  - Λ production and V^0 production ratios.
- Production of $c\bar{c}$ and $b\bar{b}$ bound states (J/ψ, $\Upsilon(n\mathrm{S})$, *etc.*)
- Measurements of b-hadron cross-sections and production fractions,
- Open charm production cross-sections.

Total $\sim 5.7\,\mathrm{pb}^{-1}$ of data collected in the $50\,\mathrm{ns}$ intensity ramp.

The first results of the effort were shown at EPS, within a week of the conclusion of data collection.

LUMINOSITY CALIBRATION WITH SMOG

The LHCb SMOG system injects gas into the beam pipe around the interaction region.

Beam-gas interactions allow the beam profiles to be imaged,

- $+$ beam currents from LHC instruments $\Rightarrow$ absolute luminosity,
- Used to calibrate scalars for the full dataset.

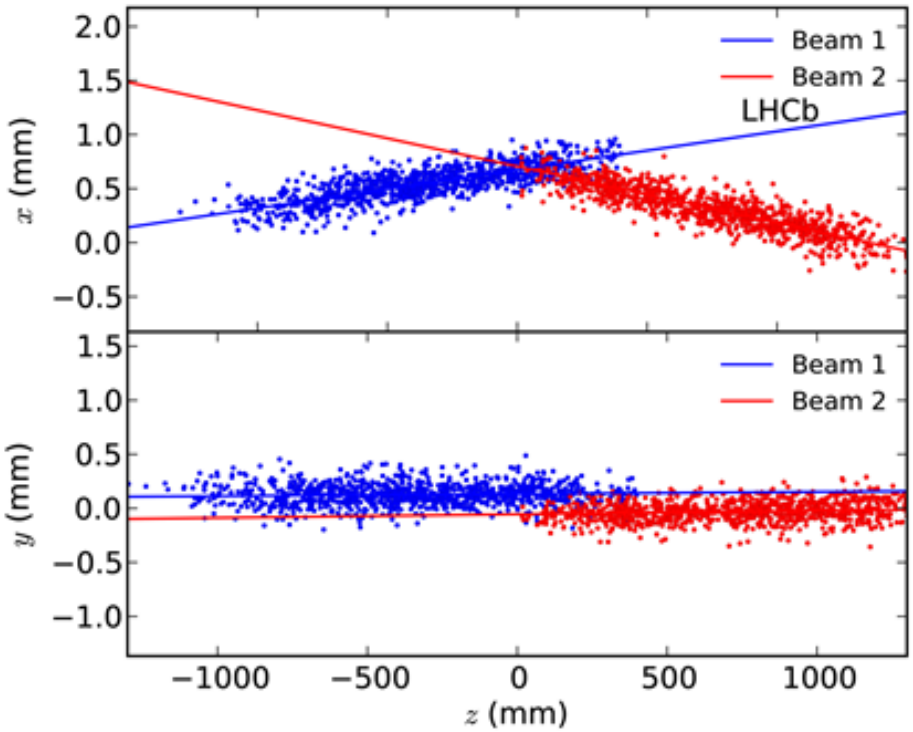

Details in JINST 9 (2014) 12, P12005.

In LHC Run 1, the combination of SMOG beam-gas imaging and Van der Meer scans gave luminosity measurements with 1.1% precision.

For the earliest Run 2 measurements, Van der Meer scan calibration is unavailable, beam-gas imaging alone gives 3.8% precision.

HEAVY FLAVOR PRODUCTION

Production measurements of heavy flavor hadrons can be vital to improved understanding of QCD,

- Test precise cross-section predictions,
- Provide empirical fragmentation functions,
- Probe proton structure.

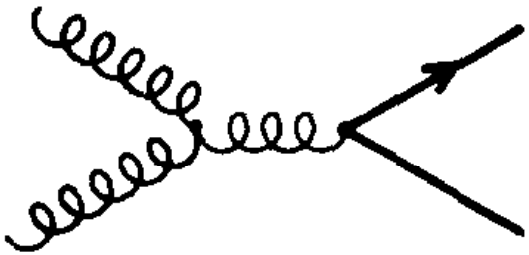

Necessary for MC generator tuning,

- Simulation inputs to precision flavor physics measurements,
- Long term program planning,
- New experiment design.

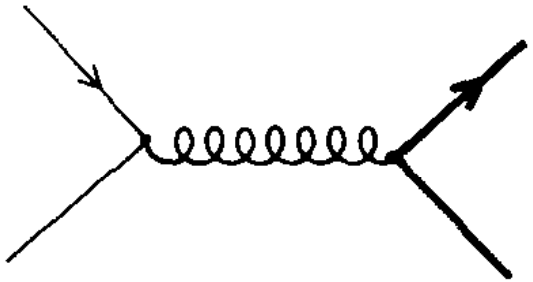

Standard Model backgrounds for New Physics searches,

- Absolute rates of SM processes must be known precisely.

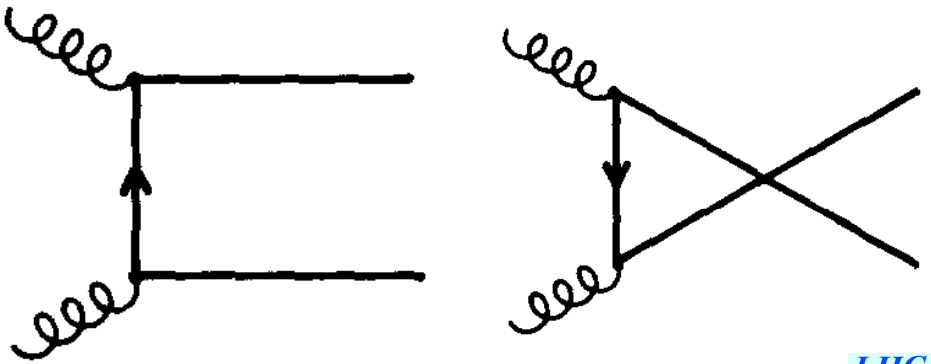

HEAVY PRODUCTION AND PROTON STRUCTURE

Heavy flavor forward production in LHC proton-proton collisions primarily through gluon-gluon fusion.

LHCb flavor production measurements cover a partonic momentum fraction x complementary to the HERA DIS data,

- HERA: $10^{-4} < x \lesssim 10^{-1}$,
- LHCb: $5 \times 10^{-6} < x \lesssim 10^{-4}$.

Inclusion of LHCb data should improve precision of gluon PDFs at small x,

- Implications for lepton flux calculations in atmospheric showers.

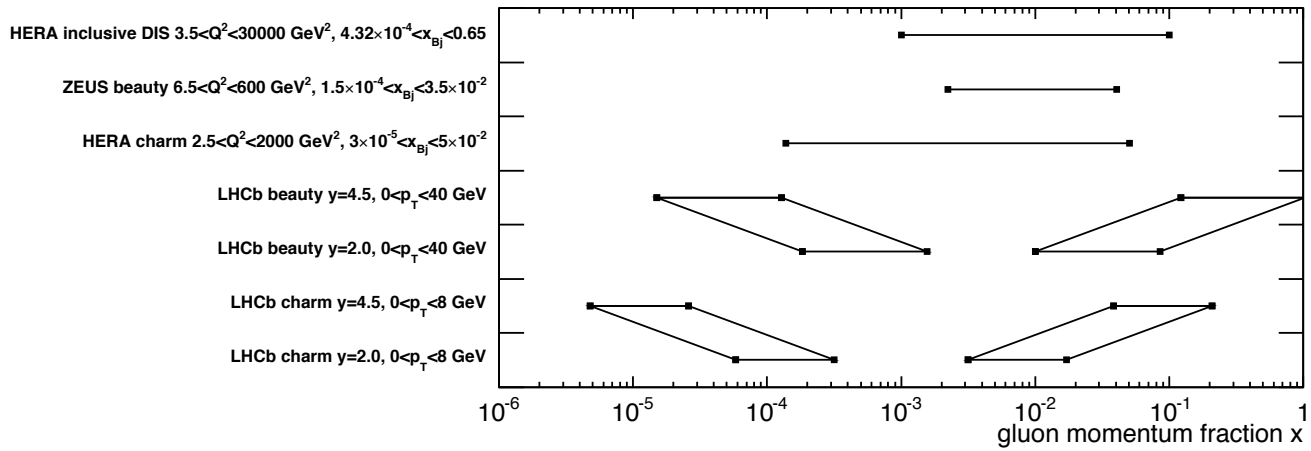

PROSA Collaboration, Eur.Phys.J. C75 (2015) 8, 396 (arXiv:1503.04581).

LHCb Run 2 dataflow

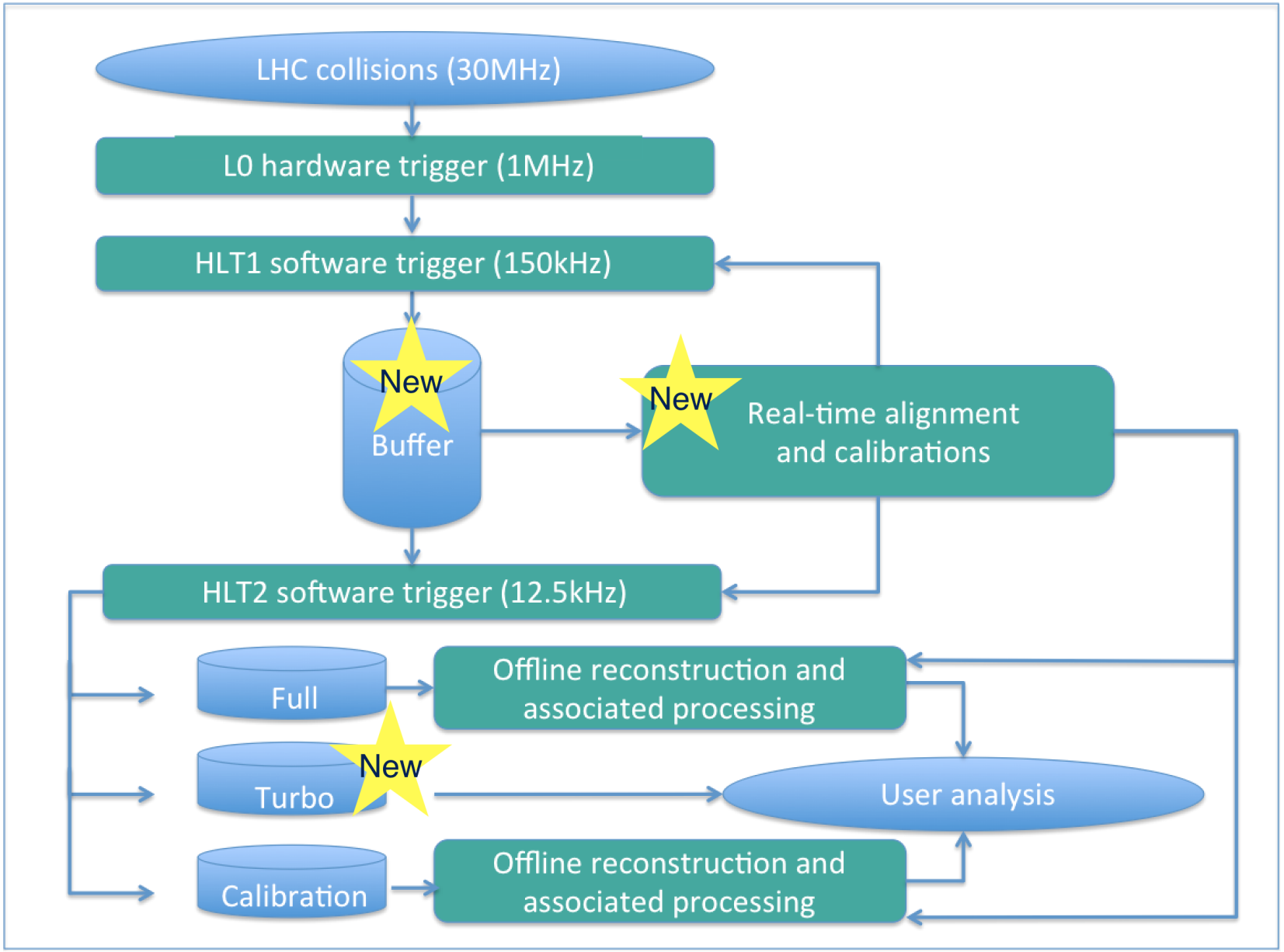

Real-time calibration

It is a matter of precision!

- Increased cross-sections and bunch-crossing rate $\Rightarrow$ event rate increase,
- HLT software trigger must be more selective than it was in LHC Run 1,
- In order to meet LHCb's need for precision, the event reconstruction in HLT2 must be as precise as offline reconstruction,
- The detector calibration must be done prior to HLT2.

Event Filter Farm has been significantly upgraded,

- $\sim$5 PB disk space,
- 27k physical cores ($\sim$55k logical cores),

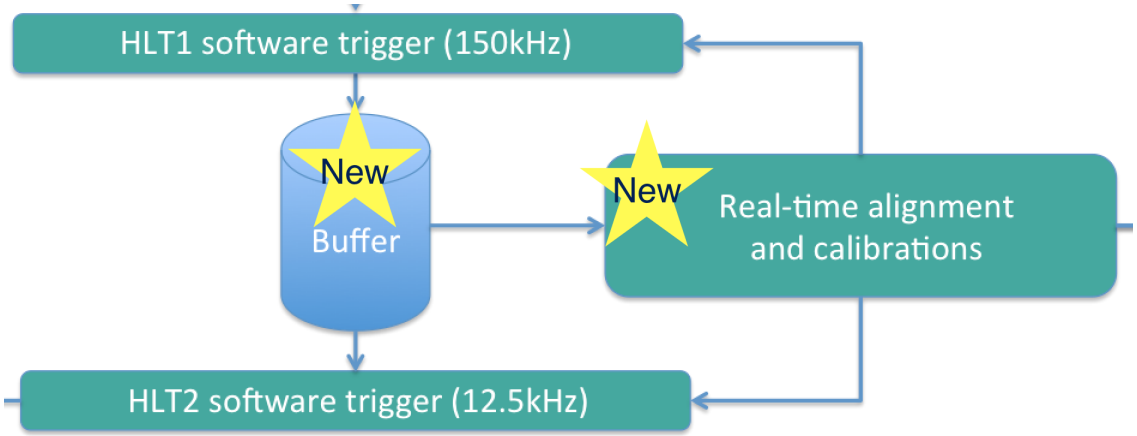

- Nodes added for Run 2 are about 2x more powerful than previous nodes.

Buffering also allows continuous use of farm throughout inter-fill.

Alignment and calibration strategy

- Automatic evaluation at regular intervals, *e.g.*, per run (typically $\sim$1 hr of data collection) or per fill, depending on task,
- Task-specific data samples selected by special triggers,
- Evaluated in minutes,
- Update alignment and calibration constants only as necessary,
- The same constants used in the HLT2 reconstruction and offline reconstruction.

Aligns $\sim$1700 detector components and computes almost $\sim$2000 calibration constants (not including calorimeter calibrations)

ALIGNMENT AND CALIBRATIONS

- VELO alignment and full alignment of tracking system,
- Straw-tube tracker drift time origin calibration,
- RICH refractive index calibration,
- RICH mirror alignment,
- Automatic calorimeter PMT voltage adjustment for detector aging,
- Muon detector alignment.

ALIGNMENT AND CALIBRATIONS

- VELO alignment and full alignment of tracking system,
- Straw-tube tracker drift time origin calibration,
- RICH refractive index calibration,
- RICH mirror alignment,
- Automatic calorimeter PMT voltage adjustment for detector aging,
- Muon detector alignment.

VELO and tracking alignment

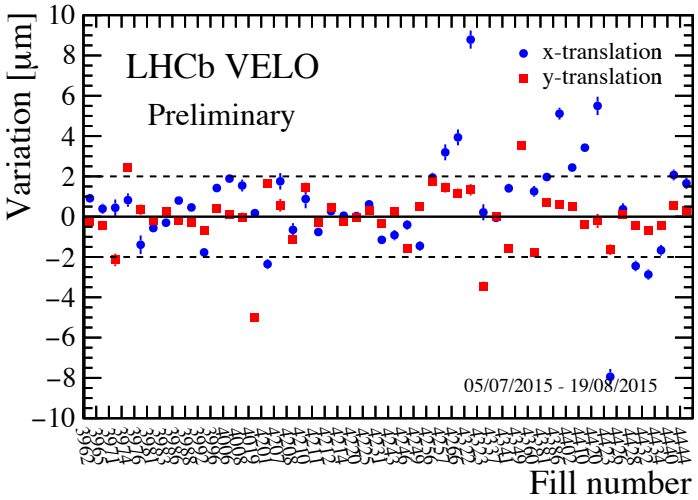

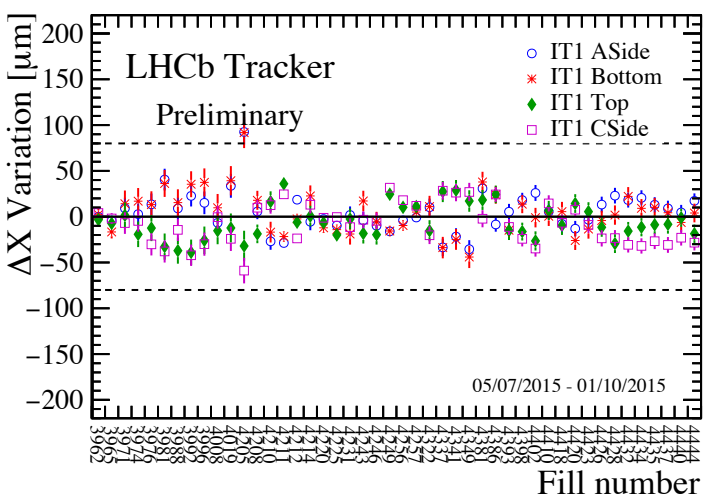

ALIGNMENT AND CALIBRATIONS

- VELO alignment and full alignment of tracking system,
- Straw-tube tracker drift time origin calibration,
- RICH refractive index calibration,
- RICH mirror alignment,
- Automatic calorimeter PMT voltage adjustment for detector aging,
- Muon detector alignment.

Drift time origin (t_0) calibration

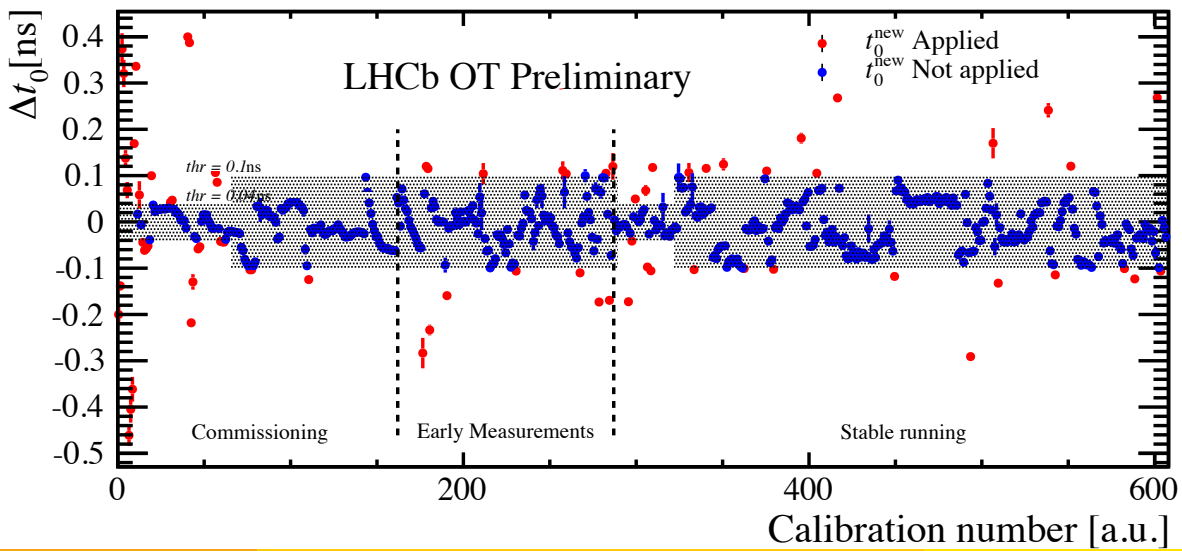

ALIGNMENT AND CALIBRATIONS

- VELO alignment and full alignment of tracking system,
- Straw-tube tracker drift time origin calibration,
- RICH refractive index calibration,
- RICH mirror alignment,
- Automatic calorimeter PMT voltage adjustment for detector aging,
- Muon detector alignment.

RICH mirror alignment

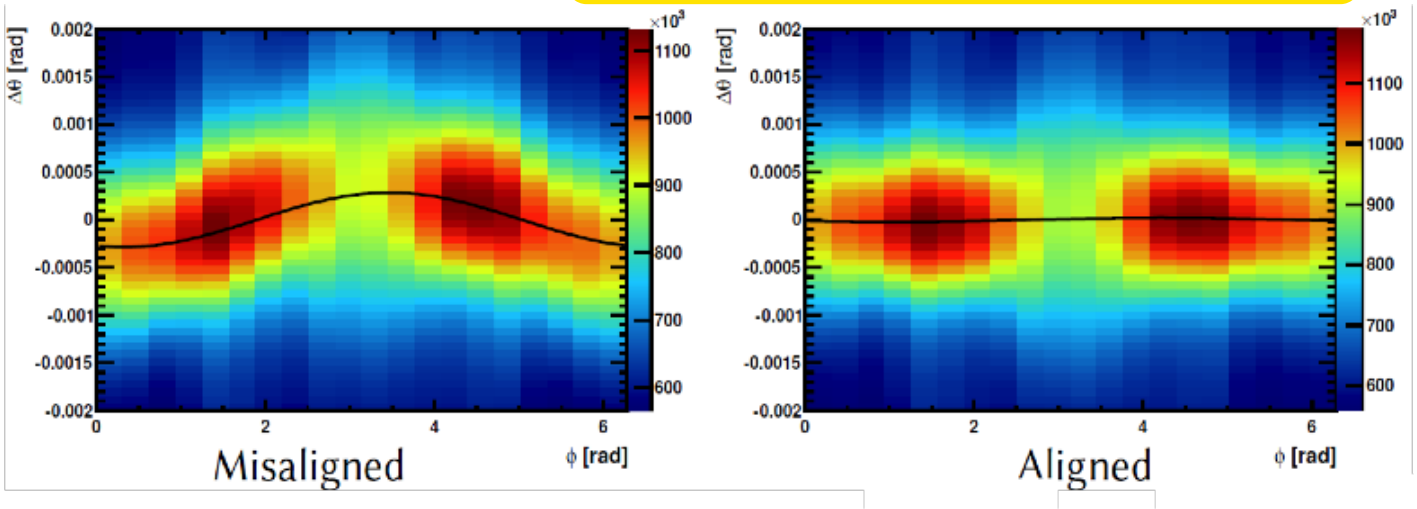

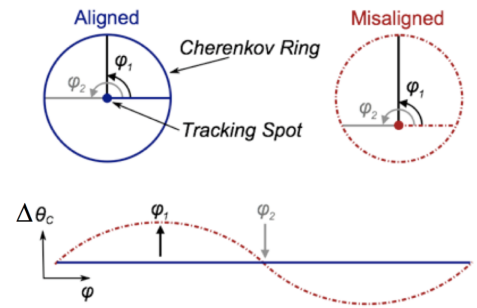

Turbo Stream

Since the HLT2 reconstruction is offline-quality, use it in analysis directly!

Complete event reconstruction in HLT2.

Reconstruction 3x faster than Run 1.

Triggers can be exclusive reconstructions of final states of interest.

In the Turbo stream, keep limited information,

- Reconstructed candidates,
- Additional information for specific measurements.

More data and greater physics reach for the same computing resources!

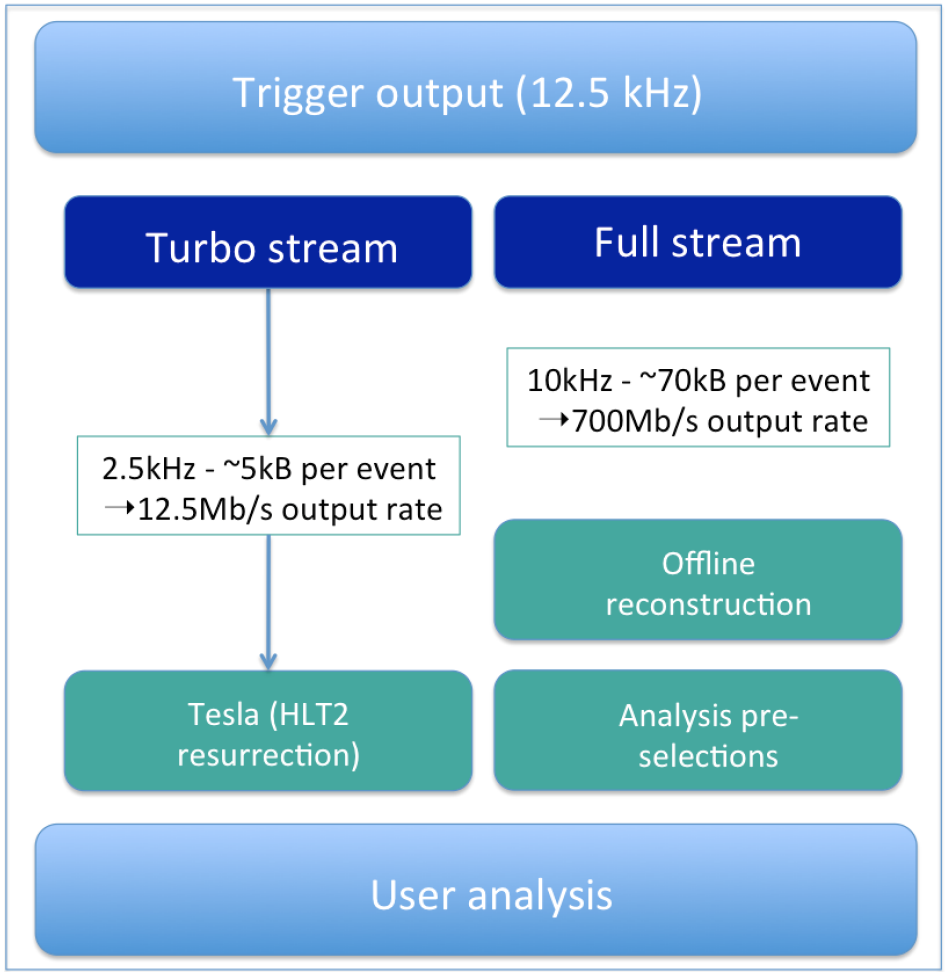

See LHCb-PROC-2015-013.

HISTORY: LHCb in 2010

When the LHC delivered the first $\sqrt{s} = 7\,\text{TeV}$ physics in 2010, production measurements were naturally among the first scientific products,

- *Measurement of charged particle multiplicities in pp collisions at* $\sqrt{s} = 7\,\text{TeV}\ldots$, Eur.Phys.J. C72 (2012) 1947, 3 million events.
- *Measurement of* V^0 *production ratios in pp collisions at* $\sqrt{s} = 0.9$ *and* $7\,\text{TeV}$, JHEP 1108 (2011) 034, $1.8\,\text{nb}^{-1}$.
- *Measurement of* J/ψ *production in pp collisions at* $\sqrt{s} = 7\,\text{TeV}$, Eur.Phys.J. C71 (2011) 1645, $5.2\,\text{pb}^{-1}$.
- *Prompt charm production in pp collisions at* $\sqrt{s} = 7\,\text{TeV}$, Nucl.Phys. B871 (2013) 1-20, $15\,\text{nb}^{-1}$.
- *Measurement of* $\sigma(pp \to b\bar{b}X)$ *at* $\sqrt{s} = 7\,\text{TeV}$ *in the forward region*, Phys.Lett. B694 (2013) 209-216, $15.1\,\text{nb}^{-1}$.
- *Measurement of b-hadron production fractions in* $\sqrt{s} = 7\,\text{TeV}$ *pp collisions*, Phys.Rev. D85 (2012) 032008, $3\,\text{pb}^{-1}$.
- and more....

The Early Measurements Task Force expands on this program for $\sqrt{s} = 13\,\text{TeV}$ and facilitates and speeds analysis.

PROSA PDF FITS

PROSA collaboration incorporates LHCb production measurements into proton PDF fits.

Two approaches

- Fit absolute measured cross-sections, $\frac{d^2\sigma}{dp_T dy}$,
- Fit normalized cross-sections, $\frac{d\sigma}{dy} / \frac{d\sigma}{dy_0}$.

Significant improvement in precision at small x and small Q^2.

Much smaller theory uncertainties in fit to normalized values,

- Absolute normalization subject to large uncertainties estimated by pQCD scale variation,
- Rapidity shape is largely scale invariant.

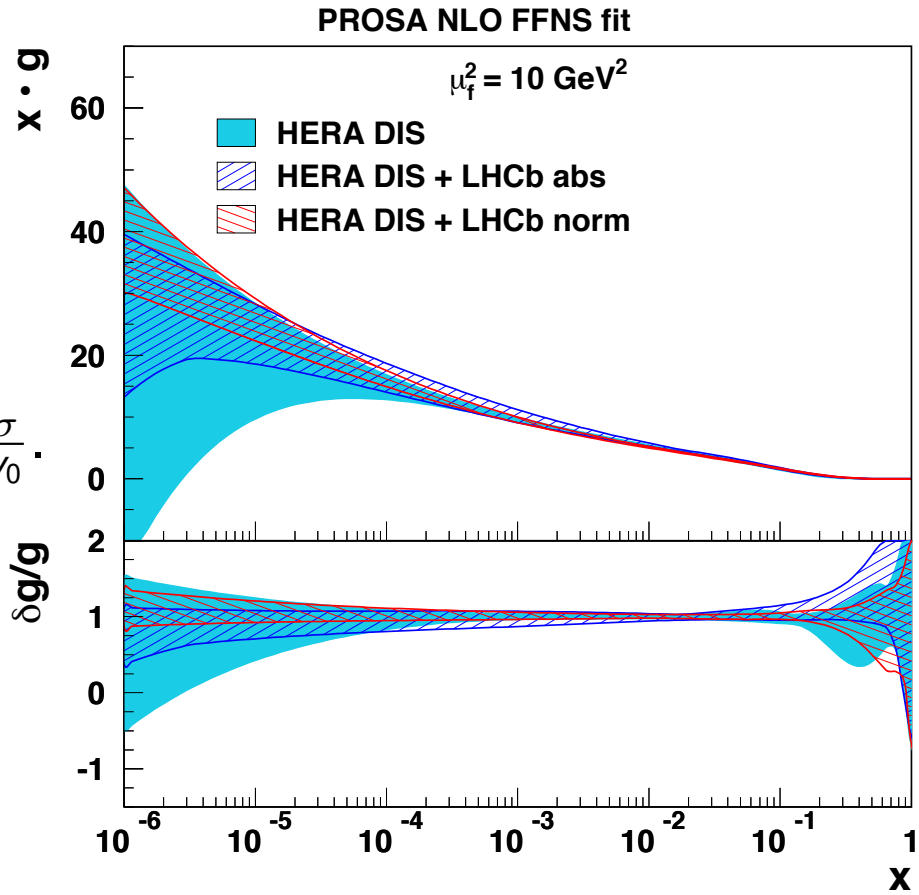

PROSA Collaboration, Eur.Phys.J. C75 (2015) 8, 396.

Incorporates LHCb D (Nucl.Phys. B871 (2013) 1-20) and B (JHEP 1308 (2013) 117) 7 TeV cross-section measurements.

CHARM AND ASTROPHYSICAL NEUTRINOS

Atmospheric charm production and decay is a dominant source of background for ultra-high-energy neutrino astrophysics.

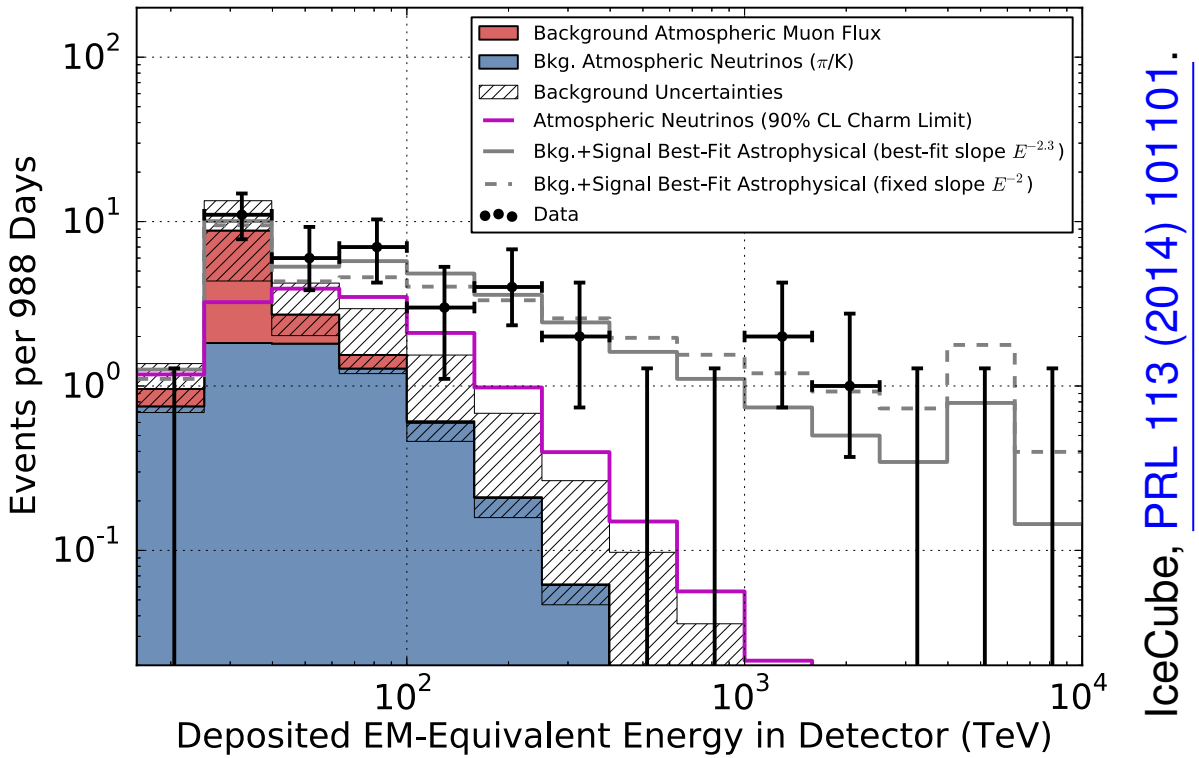

Energy of IceCube observed events with predictions of atmospheric sources and overall fit.

NEUTRINOS FROM ATMOSPHERIC CHARM

LHC measurements relevant to neutrinos from atmospheric charm production,

- *pp* at $\sqrt{s} = 7\,\text{TeV}$ (13 TeV) corresponds to incoming cosmic ray of $E = 26\,\text{PeV}$ (90 PeV).

Gauld *et al.* performed a PDF improvement similar to PROSA,

- NNPDF3.0 NLO set reweighted to match LHCb charm cross-sections at 7 TeV.

Significant improvement in precision at small x.

Improved PDF set used in POWHEG and other MC generators,

- Charm production cross-sections in LHC $\sqrt{s} = 13\,\text{TeV}$ collisions,
- Atmospheric charm production in high-energy cosmic ray interactions.

See also Bhattacharya *et al.*, JHEP 06 (2015) 110.

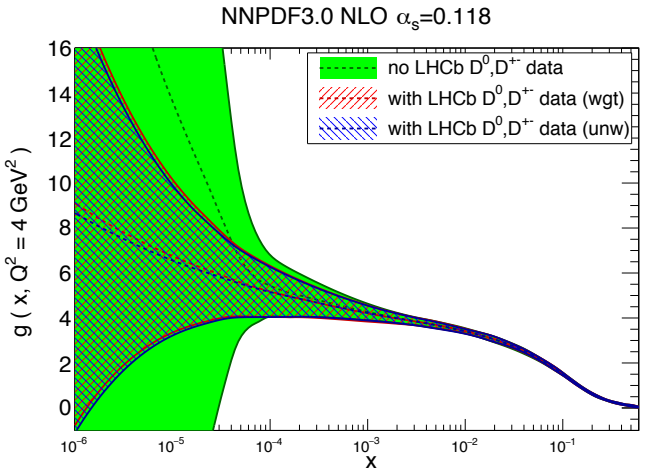

NNPDF3.0 NLO small-x gluon with LHCb charm

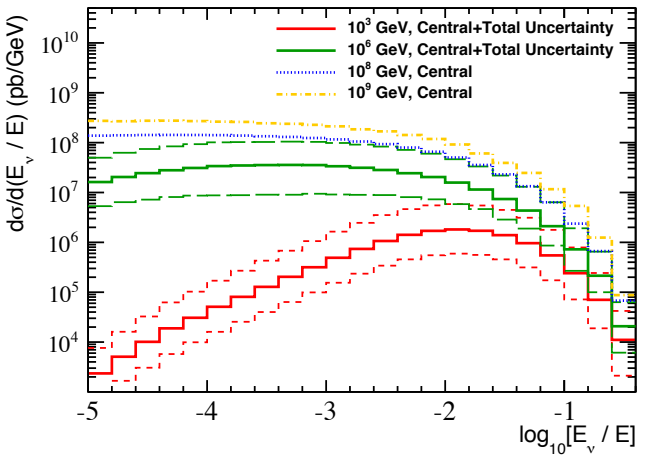

Differential cross-section of charm-induced neutrino production.

Gauld *et al.*, arXiv:1506.08025

INTRINSIC CHARM IN PROTONS

Intrinsic charm/beauty are hypothetical $c\bar{c}$ or $b\bar{b}$ contributions to the proton beyond the 'sea'.

Several potential models have been explored in theory, including five-quark $uudc\bar{c}$ states and $D^0(u\bar{c})\Lambda_c^+(udc)$ quasi-two-body bound states.

cf. pentaquarks, Phys.Rev.Lett. 115 (2015) 072001.

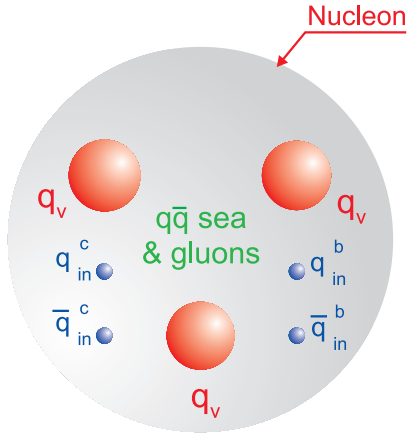

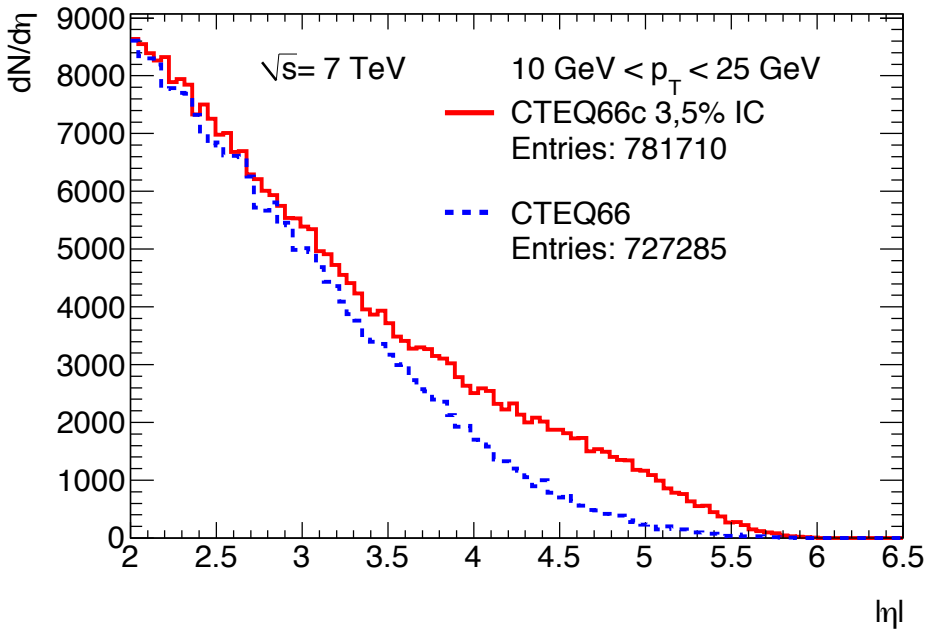

Europhys.Lett. 99 (2012) 21002 Fig. 9. Predicted $pp \to (D^0 + \bar{D}^0)X$ at $\sqrt{s} = 7$ TeV and $10 \leq p_T \leq 25$ GeV/c.

Evidence for intrinsic heavy flavor can manifest in production spectra.

Enhances forward production,

- Up to a factor of 3–10 for forward Λ_b^0 or Λ_c^+ production,
- Large enhancements in charmed meson production in ranges accessible to LHCb.

CHARM IN HADRONIC COLLISIONS

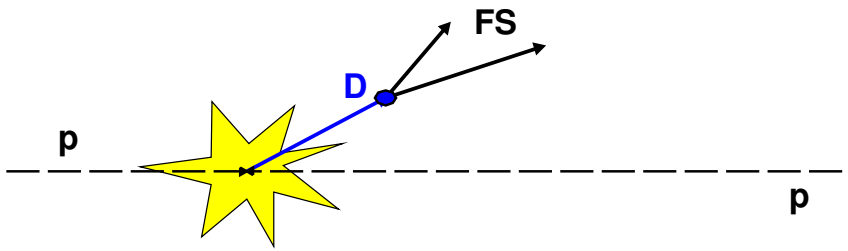

Prompt production

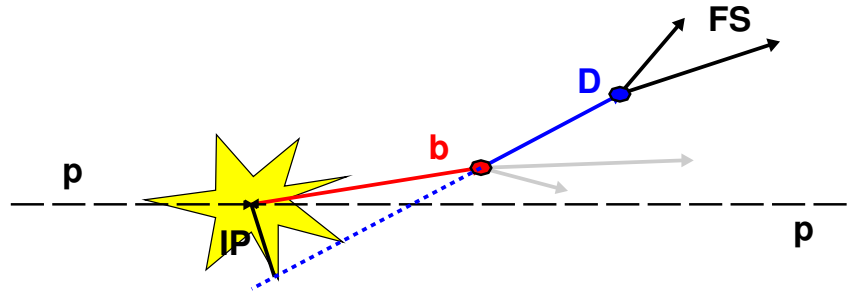

b decays ($B \to D^{(*)} X$)

Two major sources of charm:

- Prompt: Produced at primary interaction,
  - Direct production,
  - Feed-down from higher resonances.
- Secondary: Produced in the decay of a b-hadron.

Separate the prompt and secondary components,

- For J/ψ measurement, used to measure b-production cross-section,
- Secondary treated as background for D meson cross-sections.

DIFFERENTIAL CROSS-SECTIONS

Differential production cross-sections of J/ψ and D mesons (H_c),

$$\frac{\mathrm{d}^2\sigma_i(H_c)}{\mathrm{d}p_\mathrm{T}\mathrm{d}y} = \frac{1}{\Delta p_\mathrm{T}\,\Delta y} \cdot \frac{N_i(H_c \to f + \text{c.c.})}{\varepsilon_{i,\mathrm{tot}}(H_c \to f) \cdot \mathcal{B}(H_c \to f) \cdot \mathcal{L}_\mathrm{int}}$$

in bins of p_T and y with respect to the collision axis.

- $N_i(H_c \to f + \text{c.c.})$: signal yield in bin i,
- $\varepsilon_{i,\mathrm{tot}}(H_c \to f)$: total signal efficiency
  - Factorized into components, *e.g.*, track reconstruction efficiency, PID efficiency, selection efficiency, *etc.*.
  - Components evaluated in independent data samples where possible,
  - Estimated from simulation when not possible.
- $\mathcal{L}_\mathrm{int}$: integrated luminosity of sample,

HISTORY: LHCb and J/ψ forward production

LHCb has previously studied forward J/ψ production cross-sections in several collision environments,

- Enabled LHCb's excellent muon detection.

Measurement of J/ψ production in pp collisions at $\sqrt{s} = 2.76\,\text{TeV}$,
JHEP 1302 (2013) 041, $71\,\text{nb}^{-1}$.

Measurement of J/ψ production in pp collisions at $\sqrt{s} = 7\,\text{TeV}$,
Eur.Phys.J. C71 (2011) 1645, $5.2\,\text{pb}^{-1}$.

Production of J/ψ and Υ mesons on pp collisions at $\sqrt{s} = 8\,\text{TeV}$,
JHEP 1306 (2013) 064, $18\,\text{pb}^{-1}$.

J/ψ mass peak in $\sqrt{s} = 7\,\text{TeV}$ pp collisions
LHCb, Eur.Phys.J. C71 (2011) 1645.

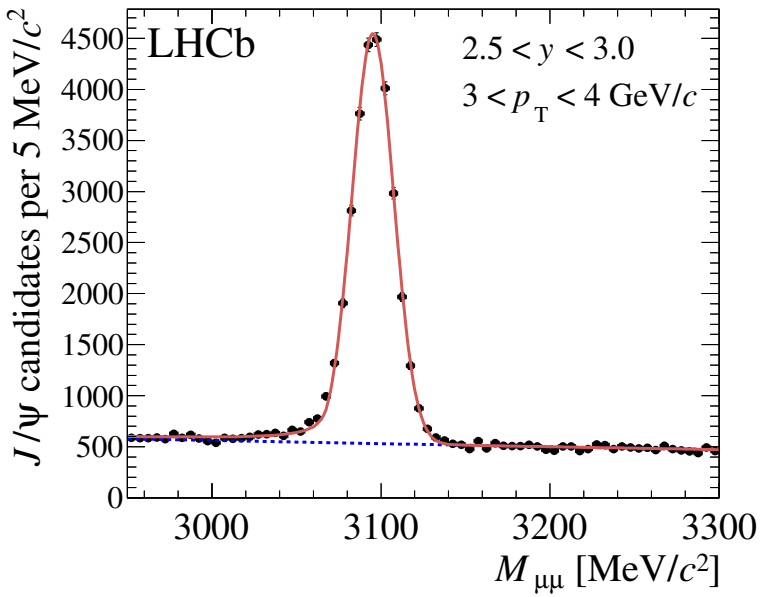

Study of J/ψ production and cold nuclear matter effects in pPb collisions at $\sqrt{s_{NN}} = 5\,\text{TeV}$,
JHEP 1402 (2014) 072, $1.6\,\text{nb}^{-1}$.

J/ψ CROSS-SECTIONS

Integrated luminosity of $3.05 \pm 0.12\,\text{pb}^{-1}$.

Analysis of HLT2 candidates with Turbo stream.

Separation of prompt J/ψ and J/ψ form b with pseudo-decay time

$$t_z = \frac{(z_{J/\psi} - z_{\text{PV}})M_{J/\psi}}{p_z}$$

Double differential cross-sections

$$\frac{\mathrm{d}^2\sigma_i(H_c)}{\mathrm{d}p_{\mathrm{T}}\mathrm{d}y}$$

for both prompt J/ψ and J/ψ from b.

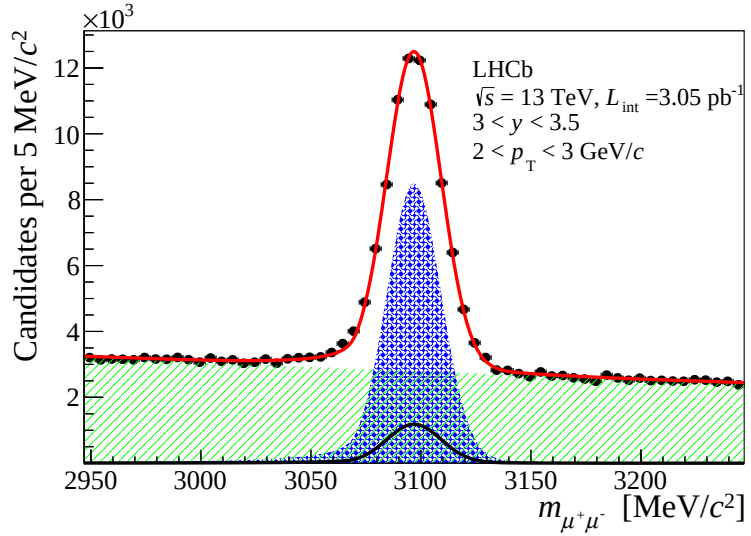

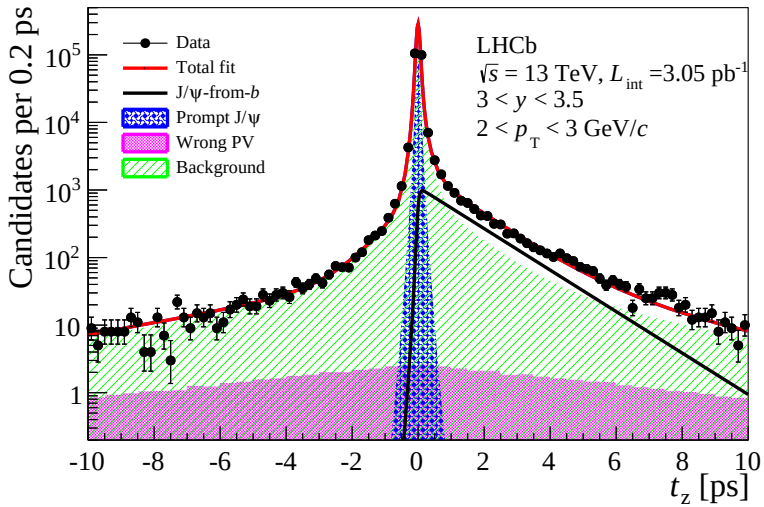

PROMPT J/ψ CROSS-SECTIONS

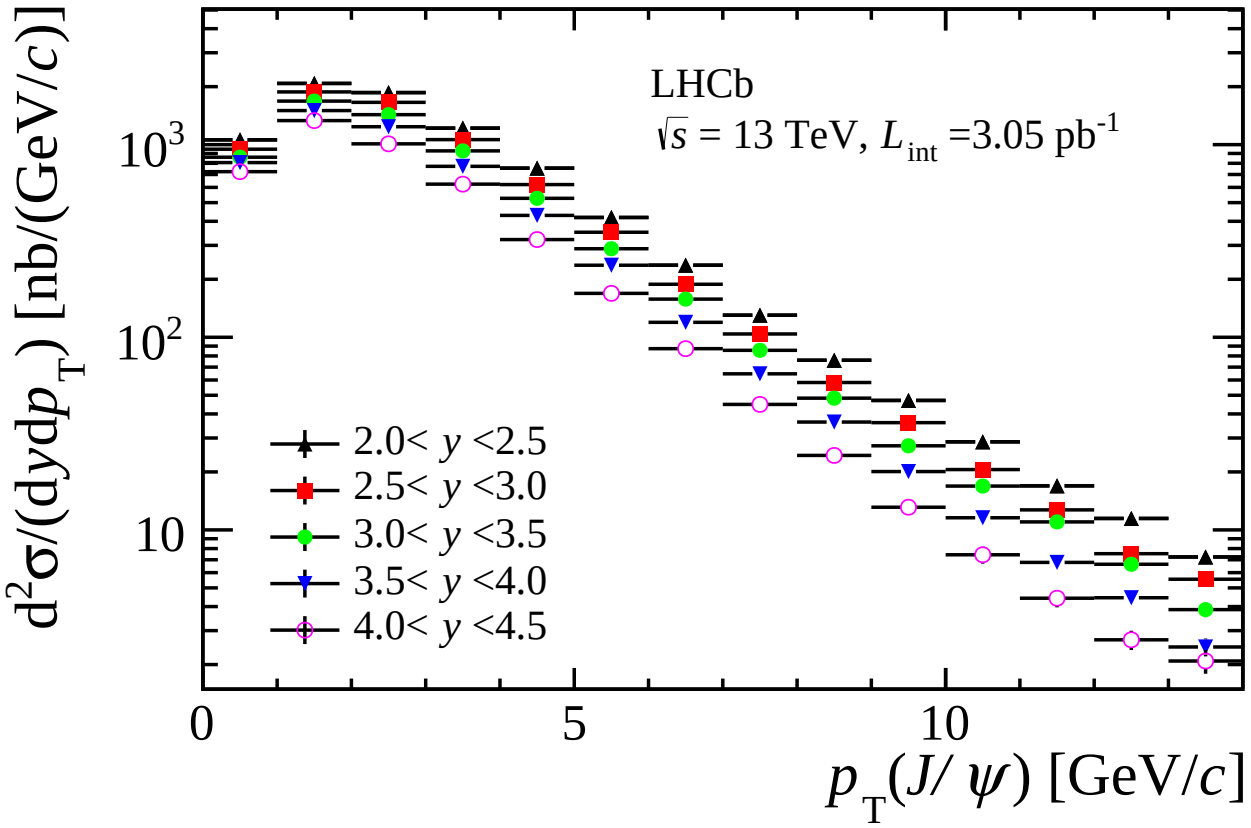

Double differential cross-sections, $d^2\sigma_i/dp_T dy$, of prompt J/ψ vs. p_T.

Integrated over the acceptance of the analysis

$$\sigma(\text{prompt } J/\psi, p_T < 14\,\text{GeV}, 2.0 < y < 4.5) = 15.30 \pm 0.03 \pm 0.86\,\mu\text{b}.$$

PROMPT J/ψ CROSS-SECTIONS

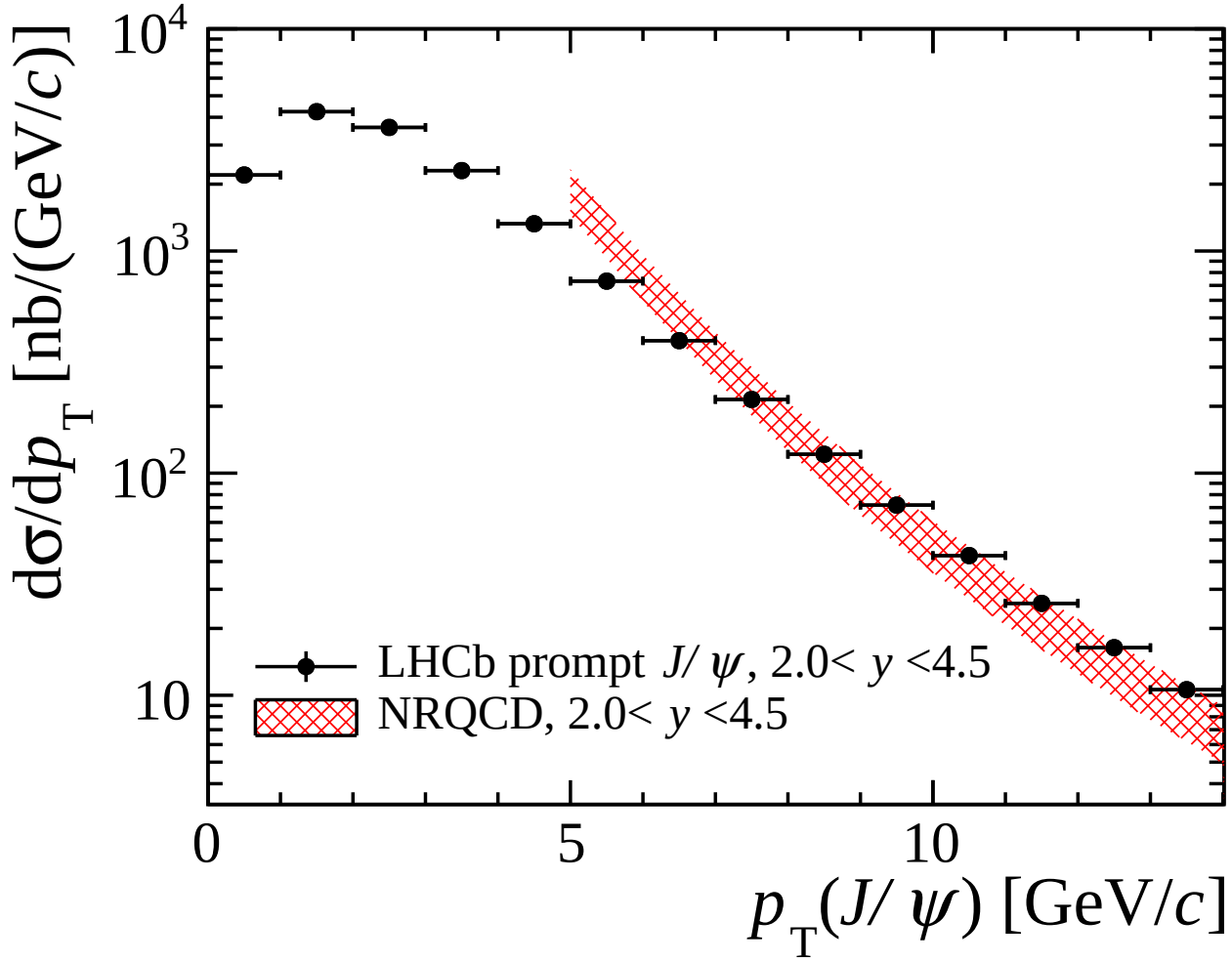

Differential cross-sections, $d\sigma_i/dp_T$, integrated over $2.0 < y < 4.5$ and compared to NRQCD calculations (Shao *et al.*, JHEP 1505 (2015) 103).

J/ψ-FROM-b CROSS-SECTIONS

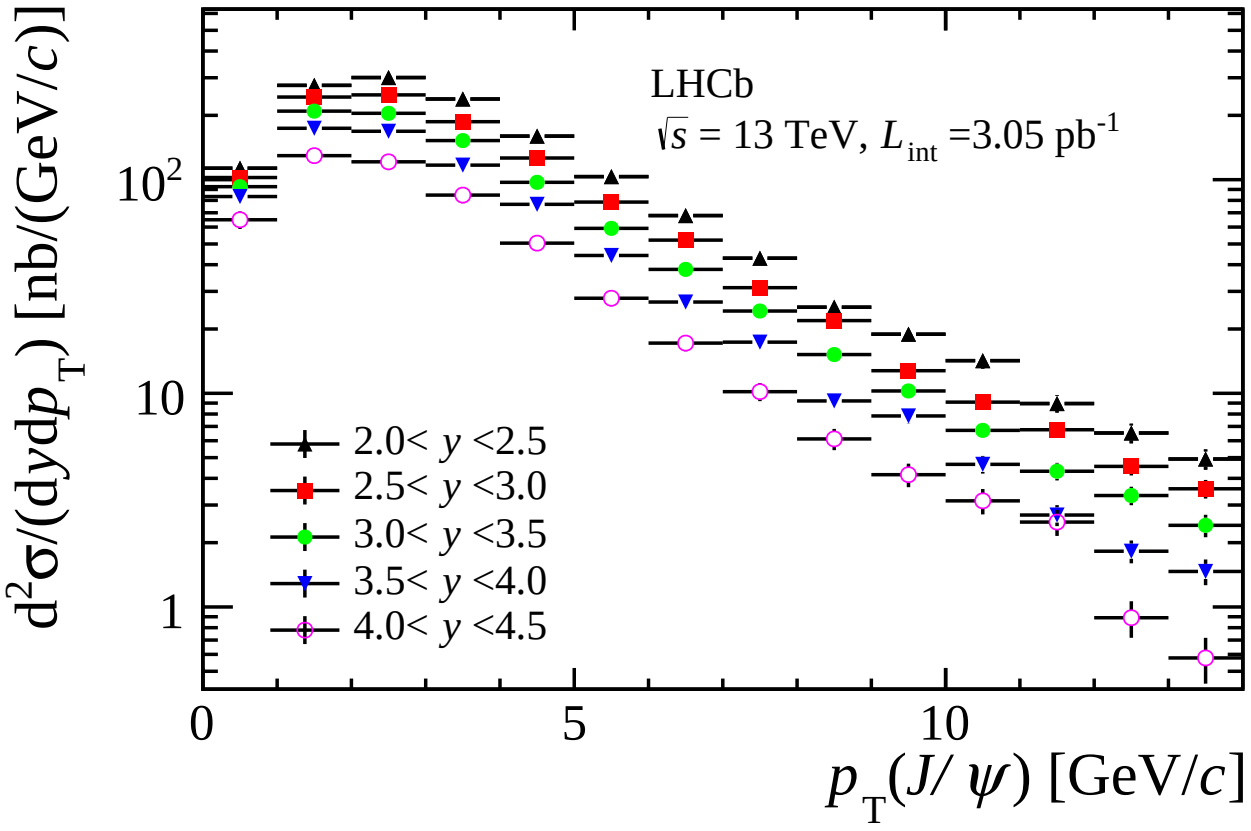

Double differential cross-sections, $d^2\sigma_i/dp_T dy$, of J/ψ-from-b vs. p_T.

Integrated over the acceptance of the analysis

$$\sigma(J/\psi\text{-from-}b, p_T < 14\,\text{GeV}, 2.0 < y < 4.5) = 2.34 \pm 0.01 \pm 0.13\,\mu\text{b}.$$

J/ψ-FROM-b CROSS-SECTIONS

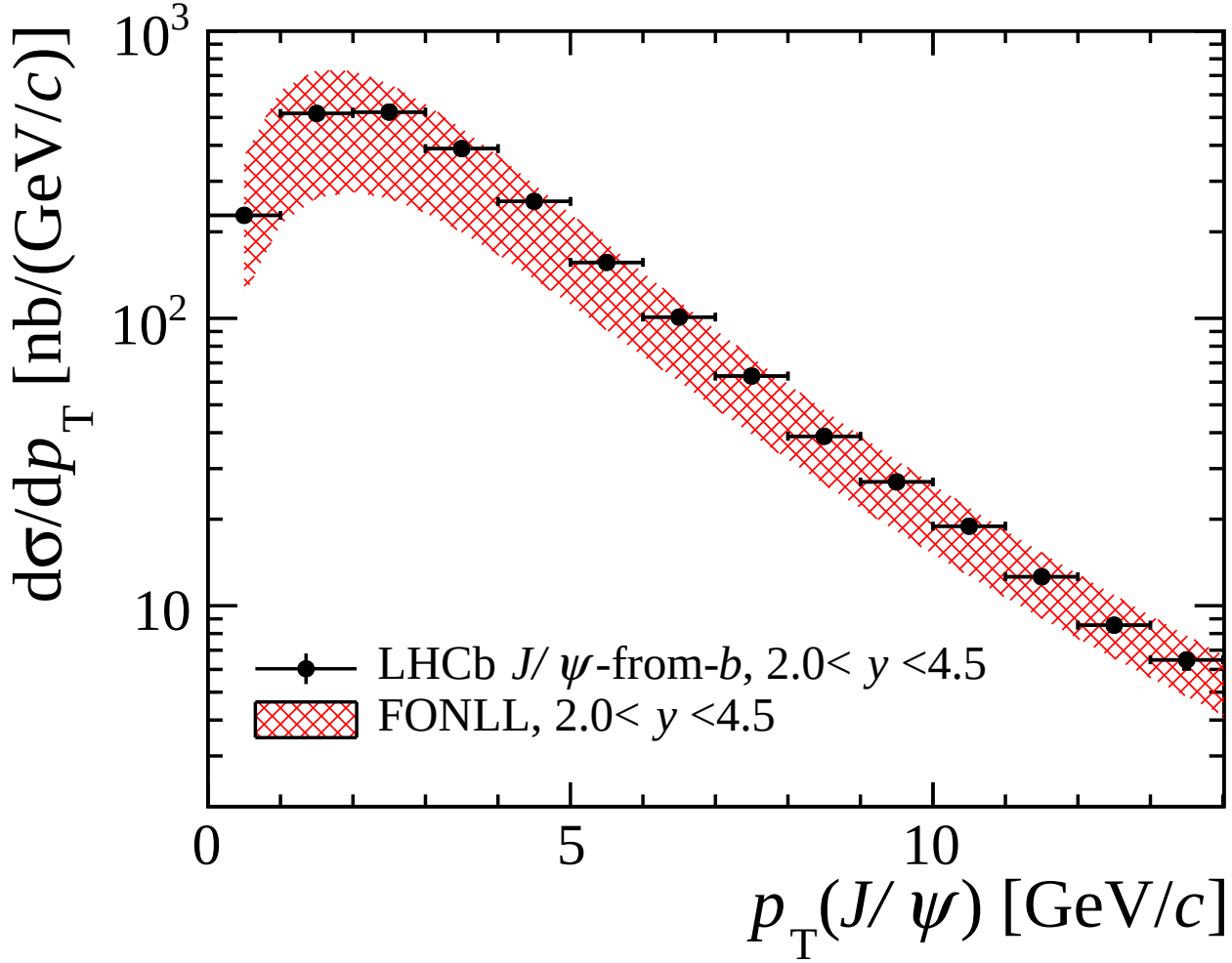

Differential cross-sections, $d\sigma_i/dp_T$, integrated over $2.0 < y < 4.5$ and compared to FONLL calculations (Cacciari *et al.*, arXiv:1507.06197).

FORWARD J/ψ CROSS-SECTION AS A FUNCTION OF $\sqrt{s}$

Prompt J/ψ production cross-sections integrated over LHCb fiducial region:

$\sigma(\text{prompt } J/\psi, \text{LHCb}, 13\,\text{TeV}) = 15.30 \pm 0.03 \pm 0.86\,\mu\text{b}.$

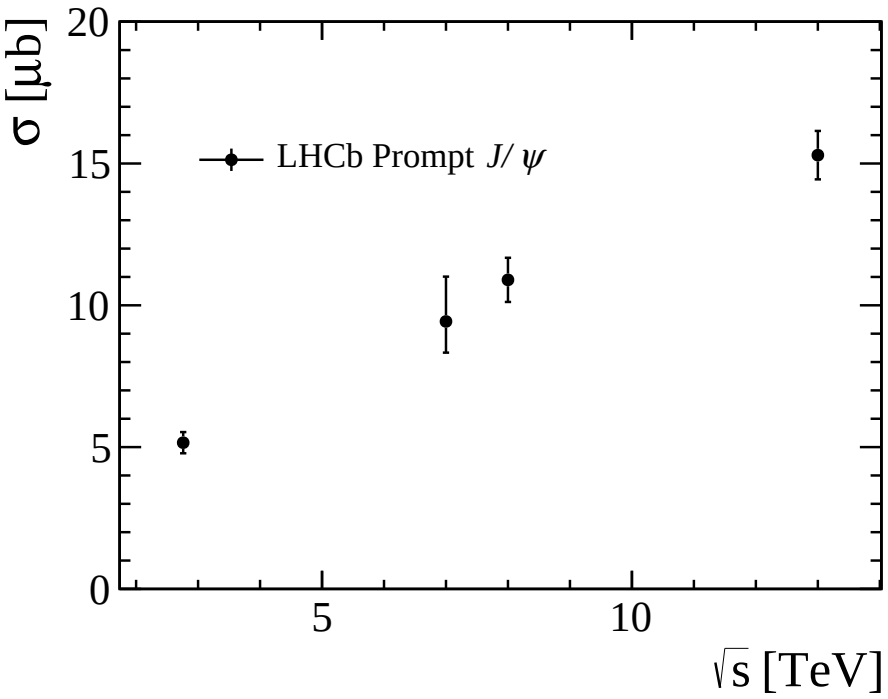

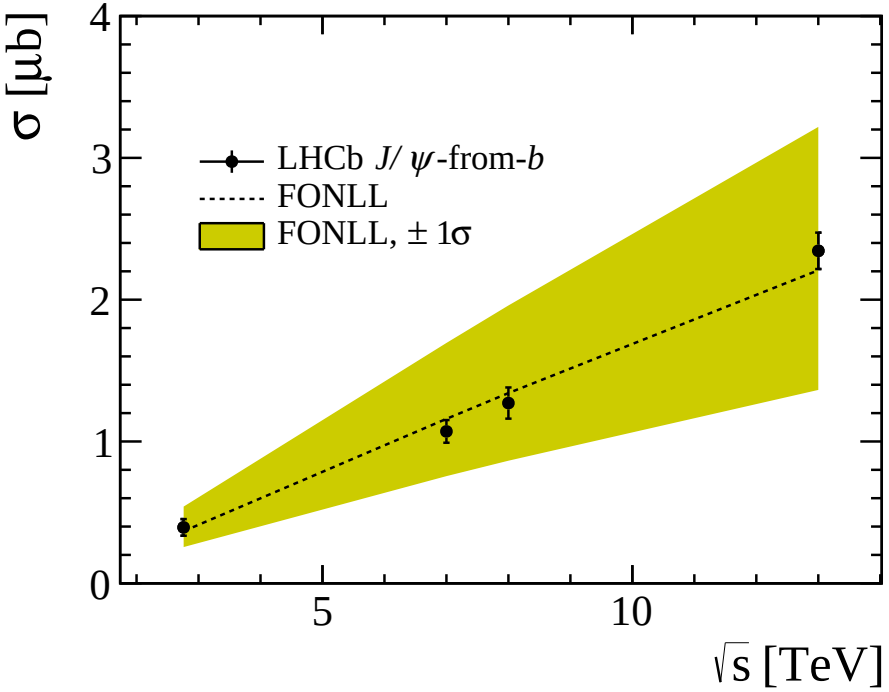

$\sigma(J/\psi\text{-from-}b, \text{LHCb}, 13\,\text{TeV}) = 2.34 \pm 0.01 \pm 0.13\,\mu\text{b}.$

Using a model based on PYTHIA6, extrapolate to a total 4π $b\bar{b}$ cross-section:

$\sigma(pp \to b\bar{b}X, 4\pi, 13\,\text{TeV}) = 515 \pm 2 \pm 53\,\mu\text{b}.$

COMPARISON WITH 8 TeV: PROMPT J/ψ

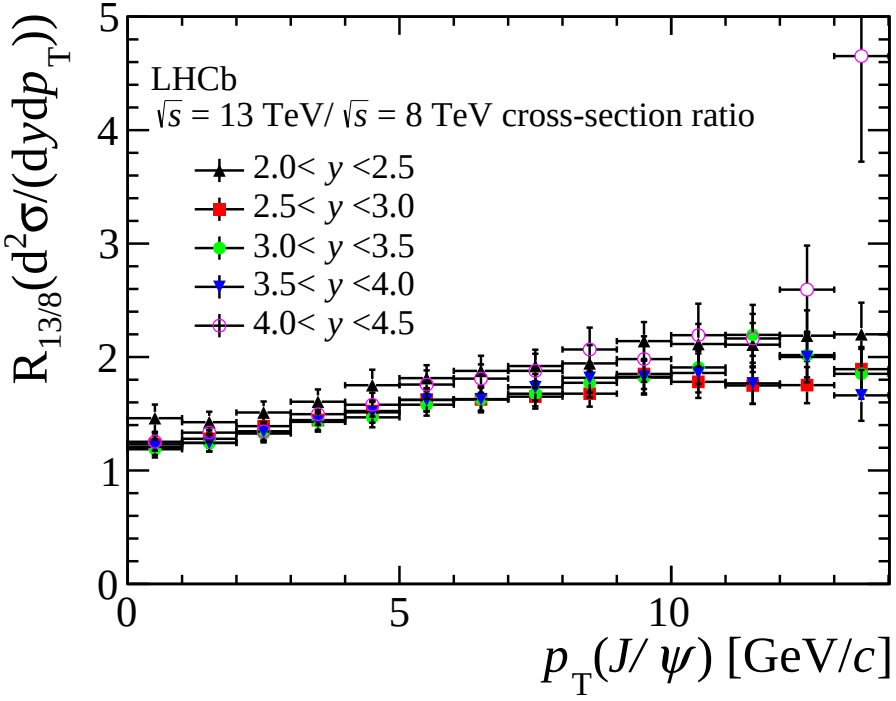

Ratios of double differential cross-sections, $\mathrm{d}^2\sigma_i/\mathrm{d}p_\mathrm{T}\mathrm{d}y$, between measurements at $\sqrt{s} = 13\,\mathrm{TeV}$ and at $\sqrt{s} = 8\,\mathrm{TeV}$.

Ratios of differential cross-sections, $\mathrm{d}\sigma_i/\mathrm{d}p_\mathrm{T}$, integrated over y between measurements at $\sqrt{s} = 13\,\mathrm{TeV}$ and at $\sqrt{s} = 8\,\mathrm{TeV}$ and compared to NRQCD calculations.

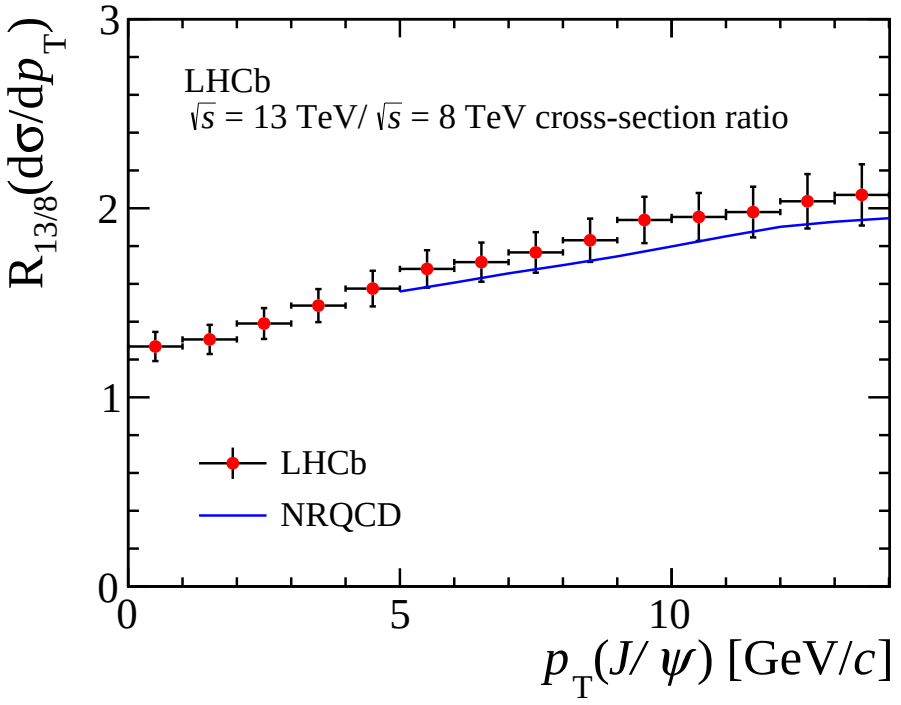

COMPARISON WITH 8 TeV: J/ψ-FROM-b

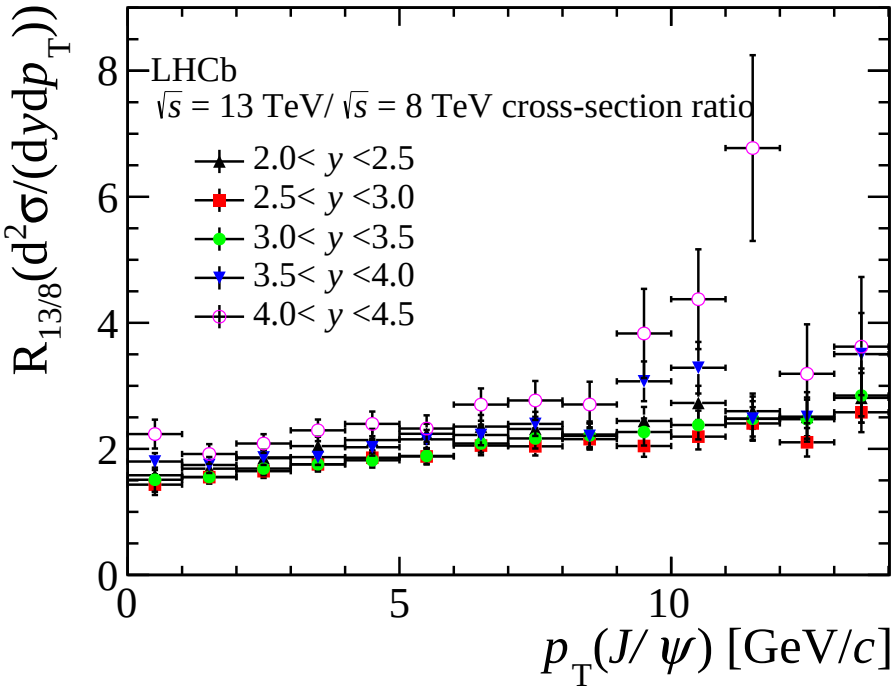

Ratios of double differential cross-sections, $\mathrm{d}^2\sigma_i/\mathrm{d}p_\mathrm{T}\mathrm{d}y$, between measurements at $\sqrt{s} = 13\,\mathrm{TeV}$ and at $\sqrt{s} = 8\,\mathrm{TeV}$.

Ratios of differential cross-sections, $\mathrm{d}\sigma_i/\mathrm{d}p_\mathrm{T}$, integrated over y between measurements at $\sqrt{s} = 13\,\mathrm{TeV}$ and at $\sqrt{s} = 8\,\mathrm{TeV}$ and compared to FONLL calculations.

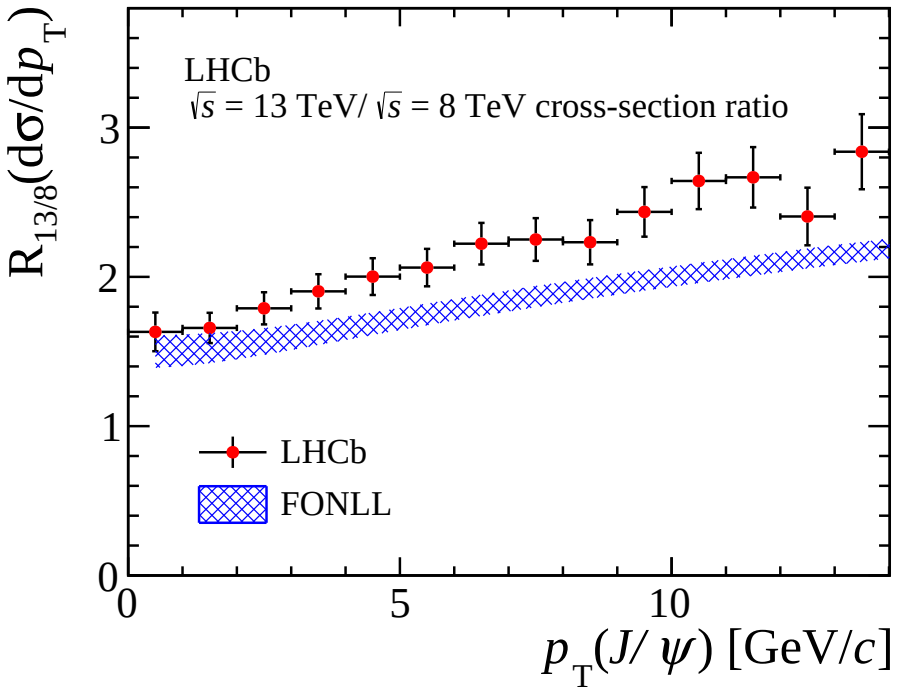

D^0, D^+, D_s^+, AND D^{*+} CROSS-SECTIONS

Integrated luminosity of $4.98 \pm 0.19\,\text{pb}^{-1}$.

Analysis of HLT2 candidates with Turbo stream.

Separation of prompt and secondary charm with $\log(IP\chi^2)$ distribution,

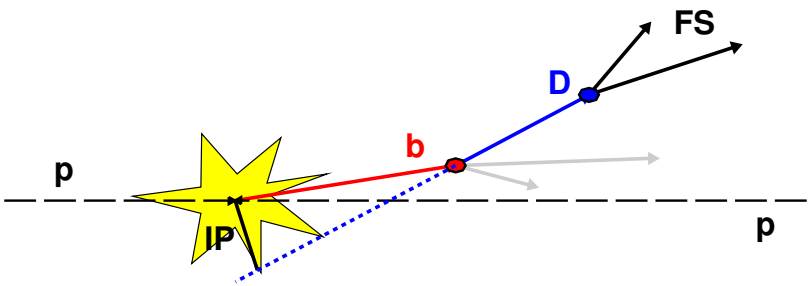

Double differential cross-sections for each meson

$$\frac{\mathrm{d}^2\sigma_i(H_c)}{\mathrm{d}p_\mathrm{T}\mathrm{d}y}$$

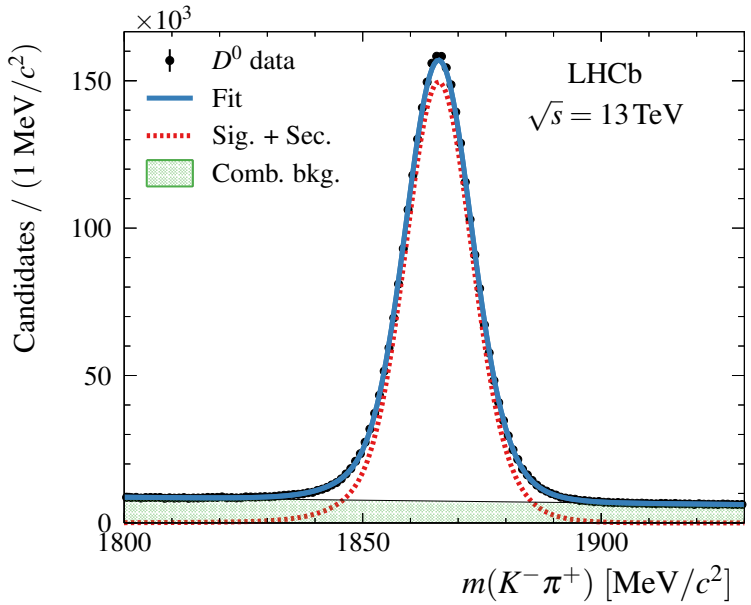

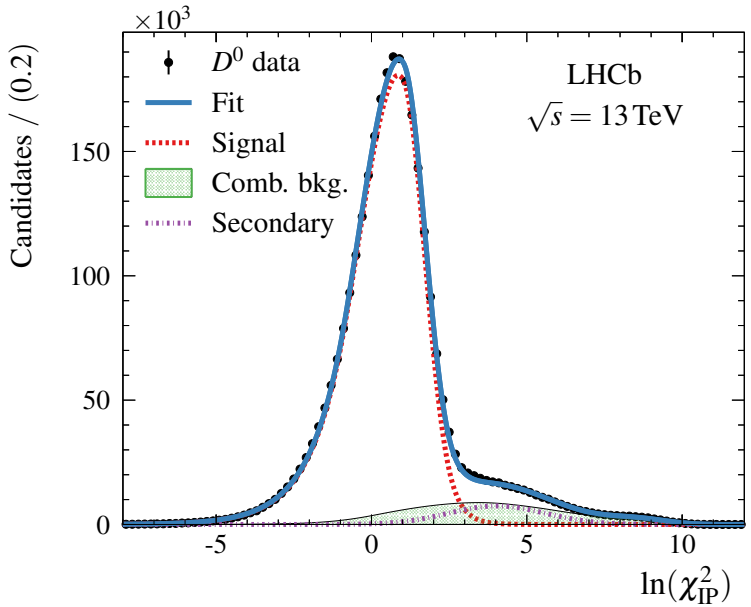

D^0, D^+, D_s^+, AND D^{*+} SIGNALS

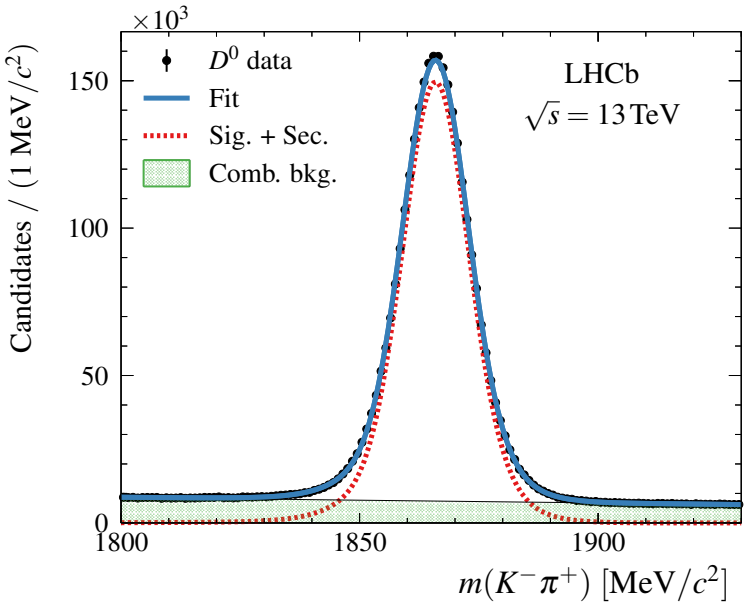

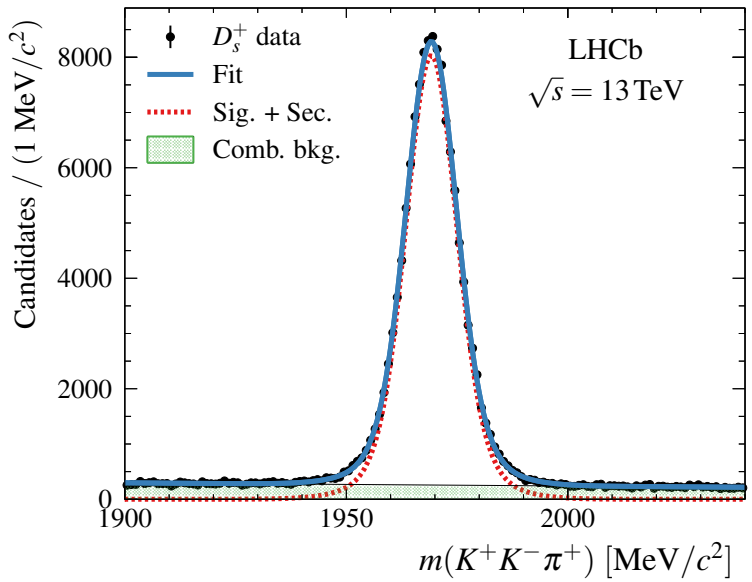

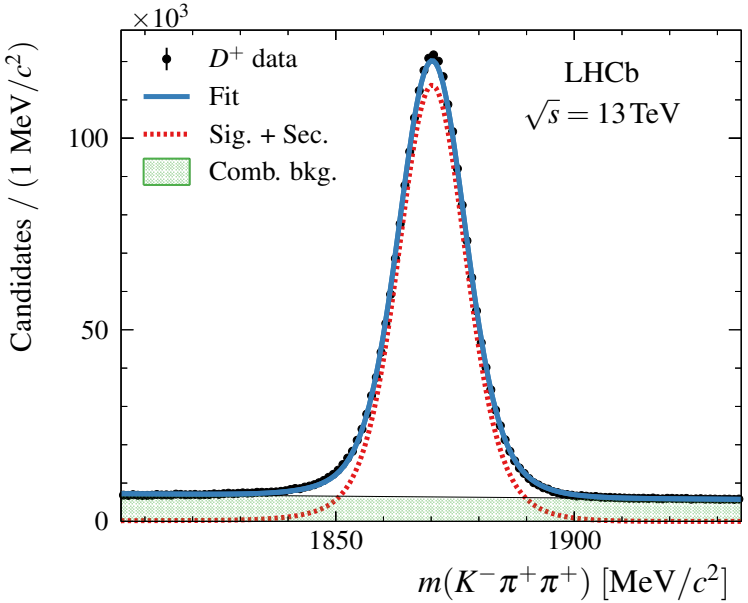

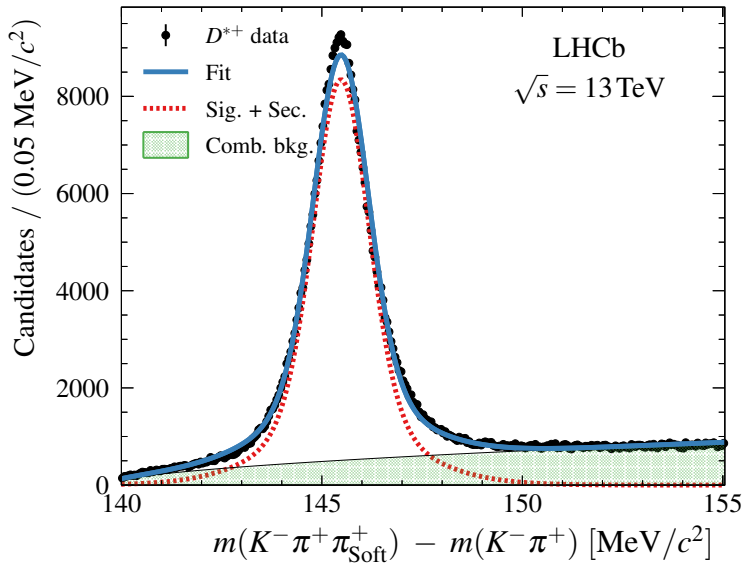

INTEGRATED $c\bar{c}$ CROSS-SECTION

The measured differential cross-sections are integrated over the analysis range

$p_{\mathrm{T}} < 8\,\mathrm{GeV}$

$2 < y < 4.5$

Integrated cross-sections are combined with fragmentation fractions measured at e^+e^- colliders.

The precise $\sigma(c\bar{c})$ estimates from the D^0 and D^+ modes are averaged.

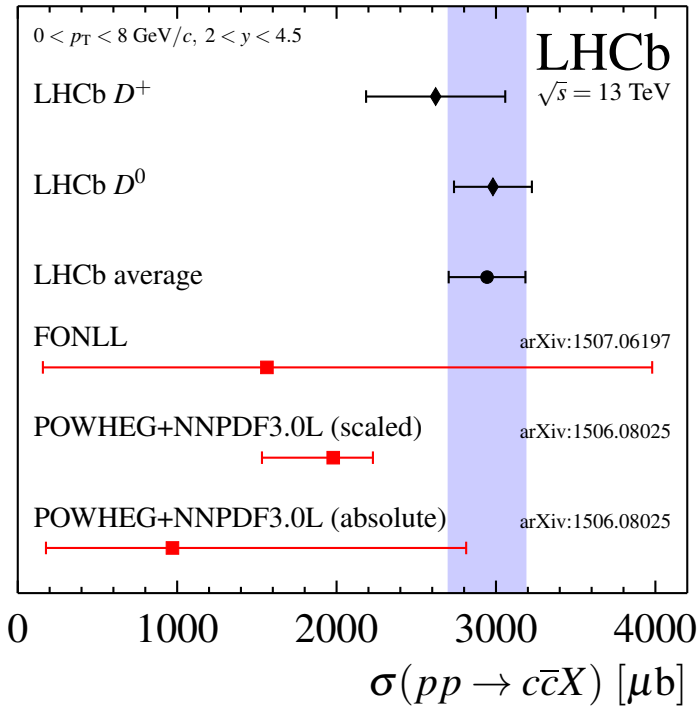

Results are compared to theoretical predictions:

- FONLL (Cacciari *et al.*, arXiv:1507.06197),
- POWHEG+NNPDF3.0L (Gauld *et al.*, arXiv:1506.08025),
- GMVFNS (Kniehl *et al.*, Eur.Phys.J. C72 (2012) 2082).

$\sigma(pp \to c\bar{c}X, p_{\mathrm{T}} < 8\,\mathrm{GeV}, 2 < y < 4.5) = 2940 \pm 3 \pm 180 \pm 160\ \mu\mathrm{b}.$

PROMPT D^0 CROSS-SECTIONS

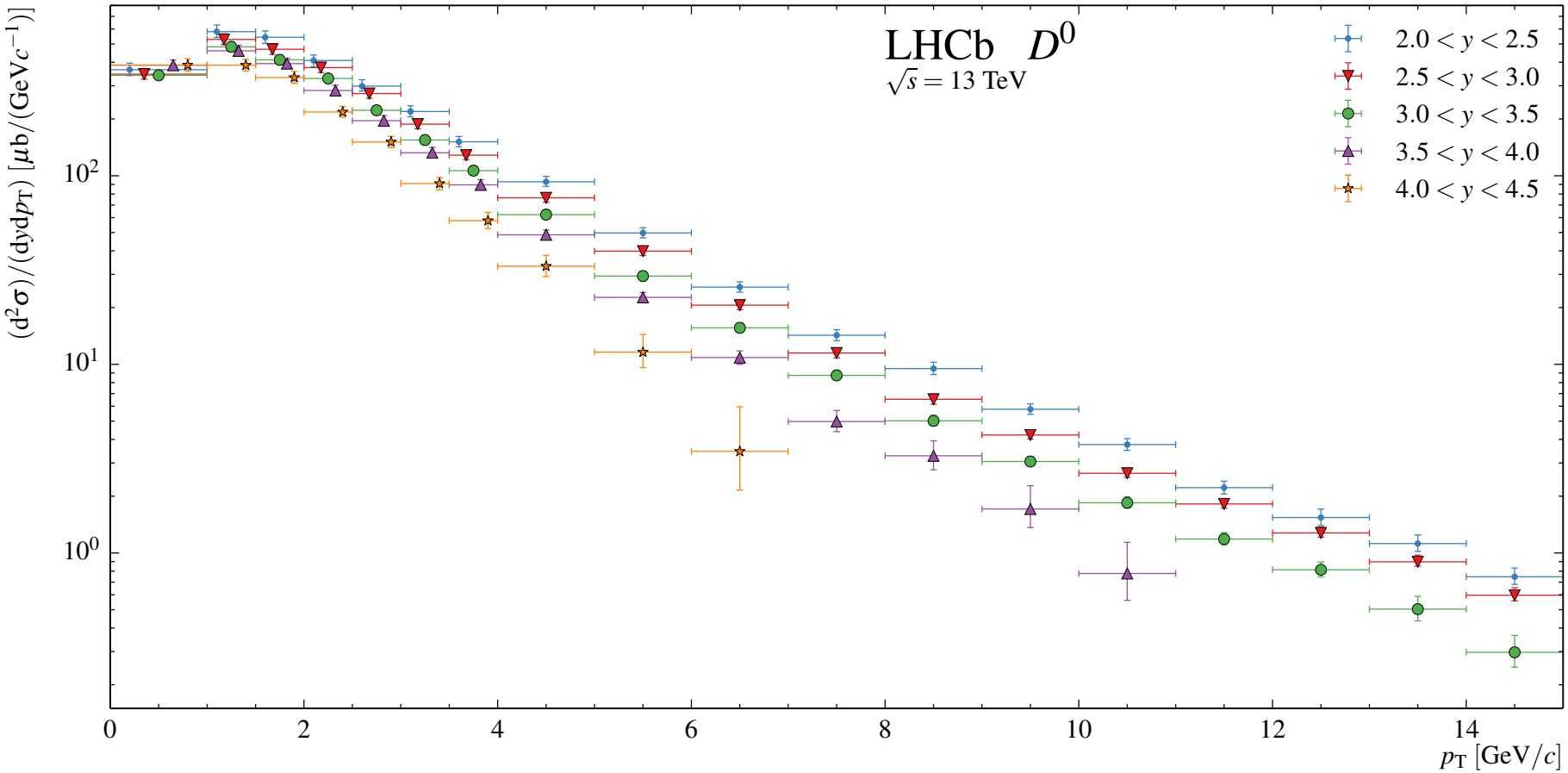

Double differential cross-sections, $d^2\sigma_i/dp_T dy$, of prompt D^0 vs. p_T.

Integrated over the acceptance of the analysis

$$\sigma(D^0, p_T < 8\,\text{GeV}, 2.0 < y < 4.5) = 3370 \pm 4 \pm 200\,\mu\text{b}.$$

PROMPT D^0 CROSS-SECTIONS

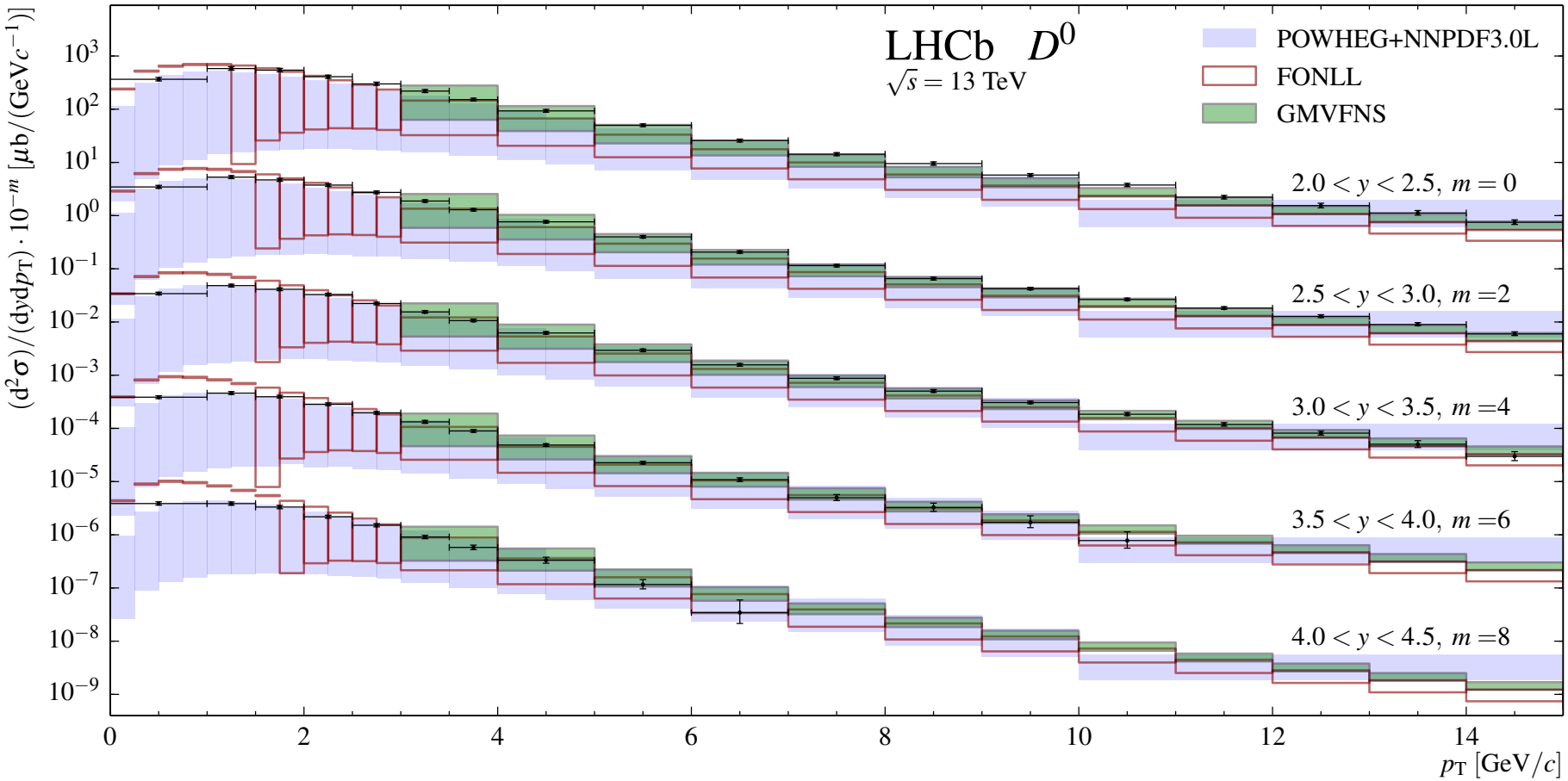

Double differential cross-sections, $\mathrm{d}^2\sigma_i/\mathrm{d}p_\mathrm{T}\mathrm{d}y$, of prompt D^0 vs. p_T.

Integrated over the acceptance of the analysis

$$\sigma(D^0, p_\mathrm{T} < 8\,\mathrm{GeV}, 2.0 < y < 4.5) = 3370 \pm 4 \pm 200\,\mu\mathrm{b}.$$

PROMPT D^+ CROSS-SECTIONS

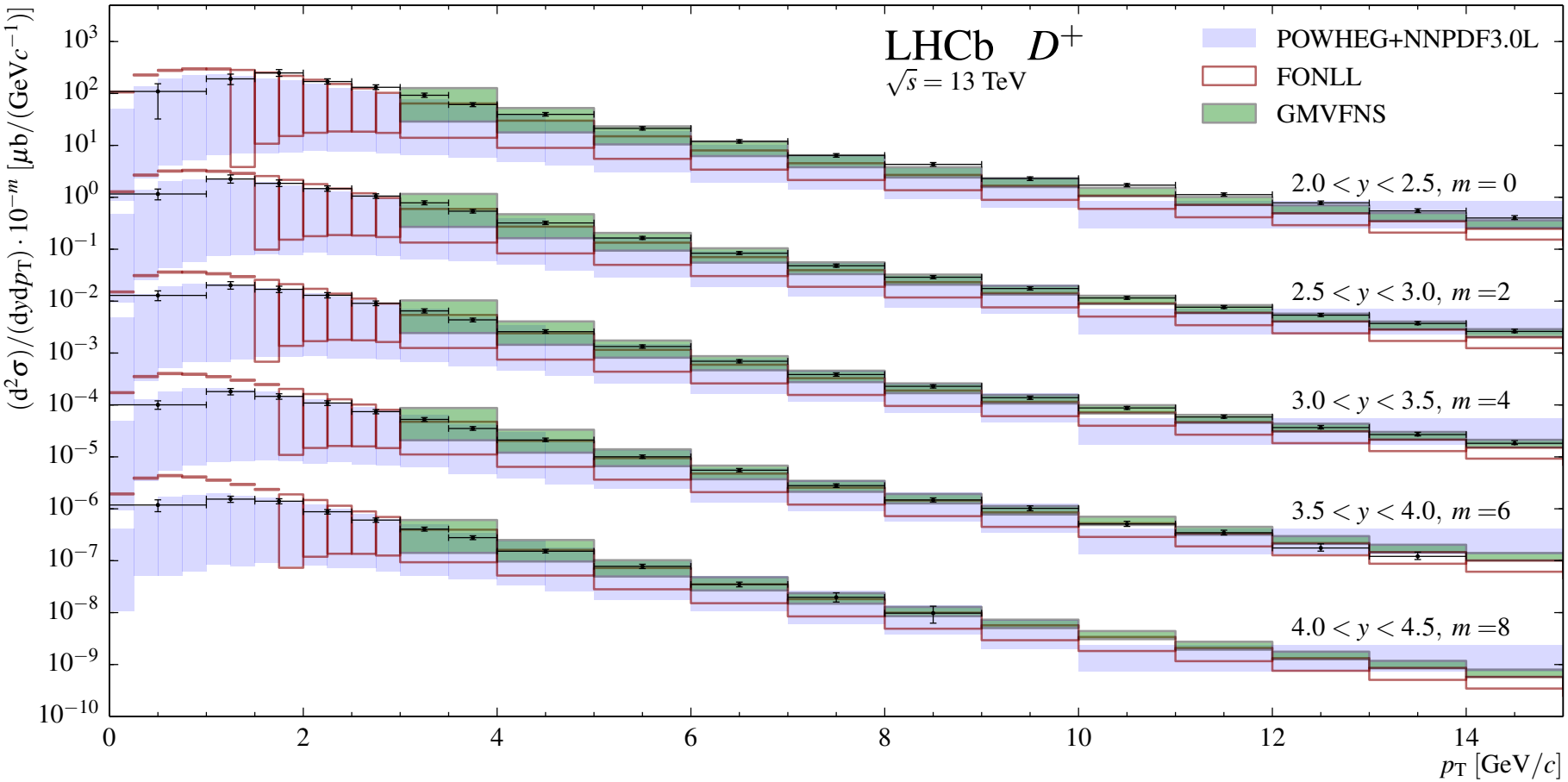

Double differential cross-sections, $\mathrm{d}^2\sigma_i/\mathrm{d}p_\mathrm{T}\mathrm{d}y$, of prompt D^+ vs. p_T.

Integrated over the acceptance of the analysis

$$\sigma(D^+, p_\mathrm{T} < 8\,\mathrm{GeV}, 2.0 < y < 4.5) = 1290 \pm 8 \pm 190\,\mu\mathrm{b}.$$

PROMPT D_s^+ CROSS-SECTIONS

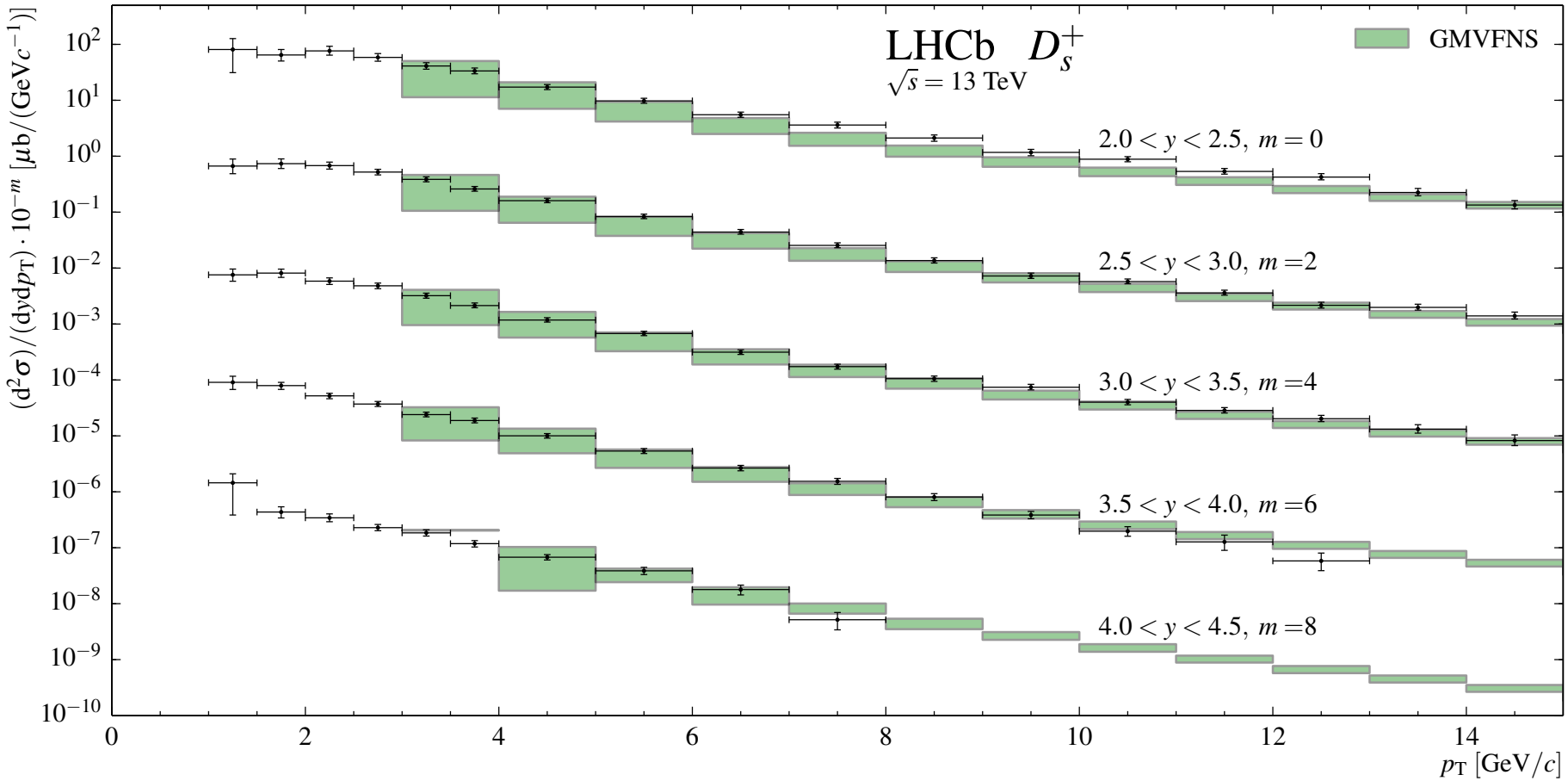

Double differential cross-sections, $\mathrm{d}^2\sigma_i/\mathrm{d}p_\mathrm{T}\mathrm{d}y$, of prompt D_s^+ vs. p_T.

Integrated over the acceptance of the analysis

$$\sigma(D_s^+, 1 < p_\mathrm{T} < 8\,\mathrm{GeV}, 2.0 < y < 4.5) = 460 \pm 13 \pm 100\,\mu\mathrm{b}.$$

PROMPT D^{*+} CROSS-SECTIONS

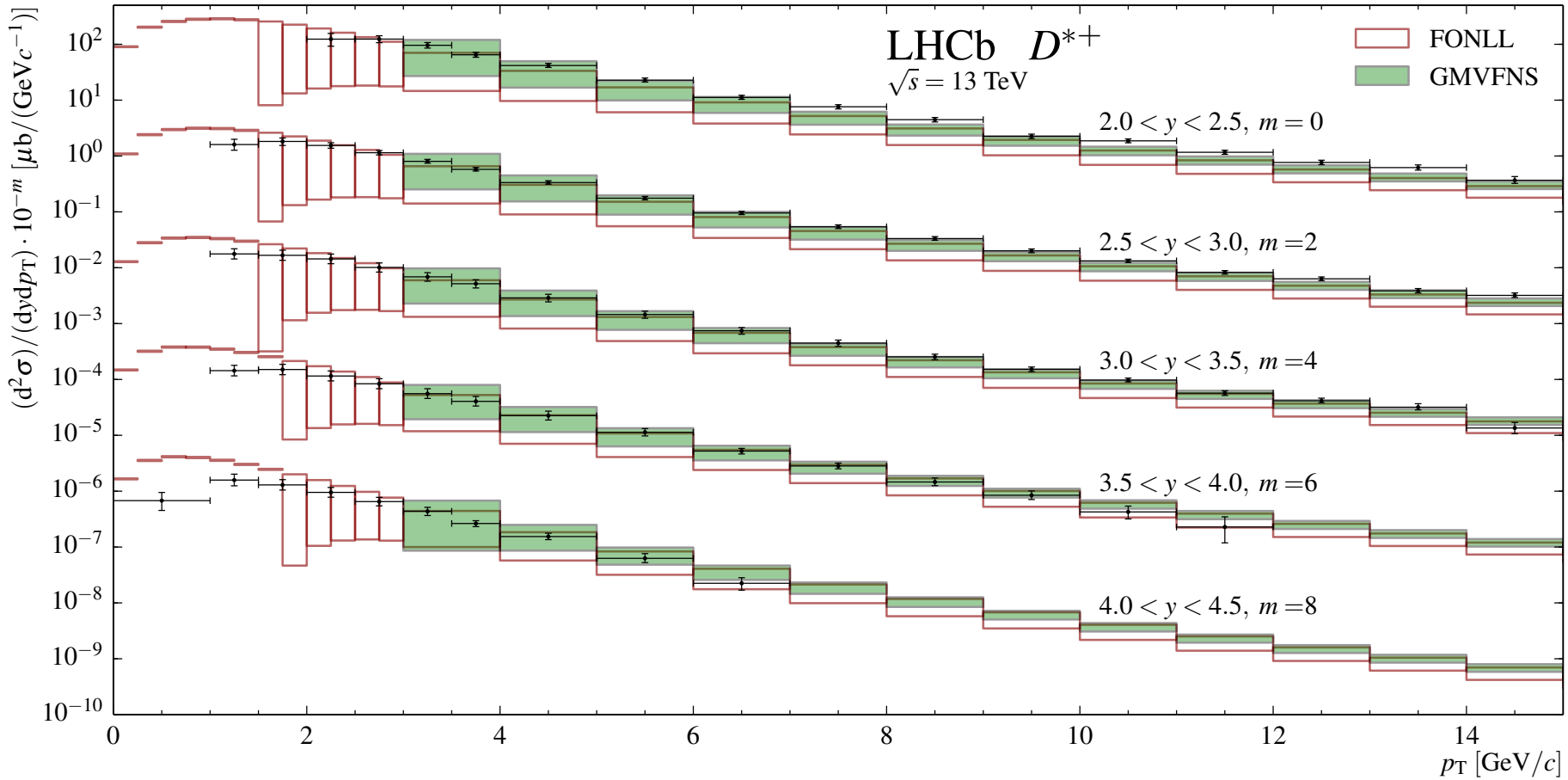

Double differential cross-sections, $d^2\sigma_i/dp_T dy$, of prompt D^{*+} vs. p_T.

Integrated over the acceptance of the analysis

$$\sigma(D^{*+}, 1 < p_T < 8\,\text{GeV}, 2.0 < y < 4.5) = 880 \pm 5 \pm 140\,\mu\text{b}.$$

COMPARISON WITH 7 TeV: D^0 AND D^+

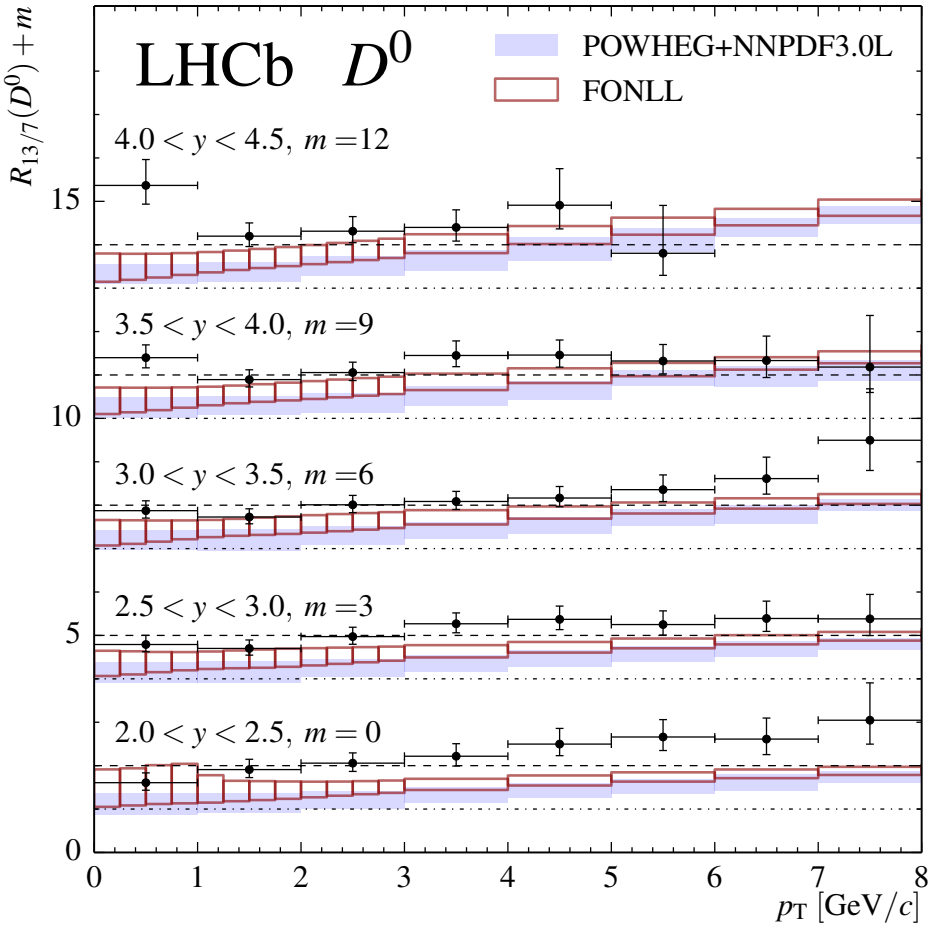

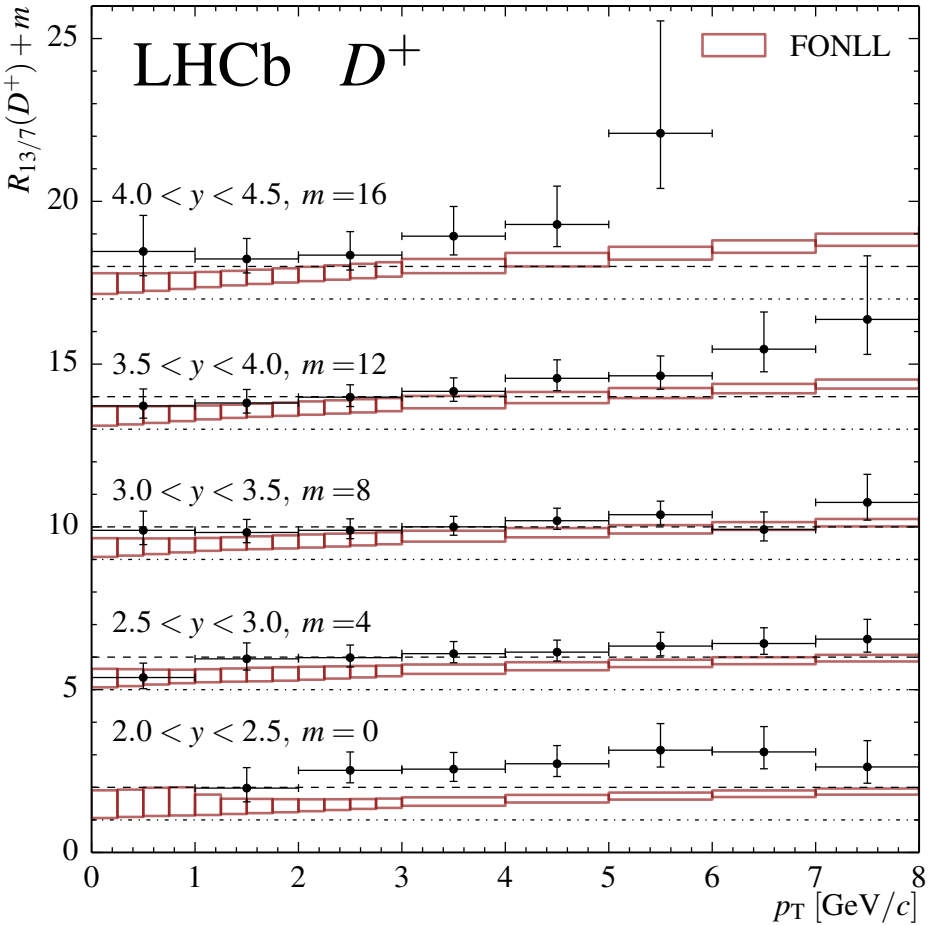

Ratios of double differential cross-sections, $\mathrm{d}^2\sigma_i/\mathrm{d}p_T\mathrm{d}y$, between measurements at $\sqrt{s} = 13\,\mathrm{TeV}$ and at $\sqrt{s} = 7\,\mathrm{TeV}$ (NPB 871 (2013) 1-20).

For each interval, the dash-dotted line represents a ratio of 1.

COMPARISON WITH 7 TeV: D_s^+ AND D^{*+}

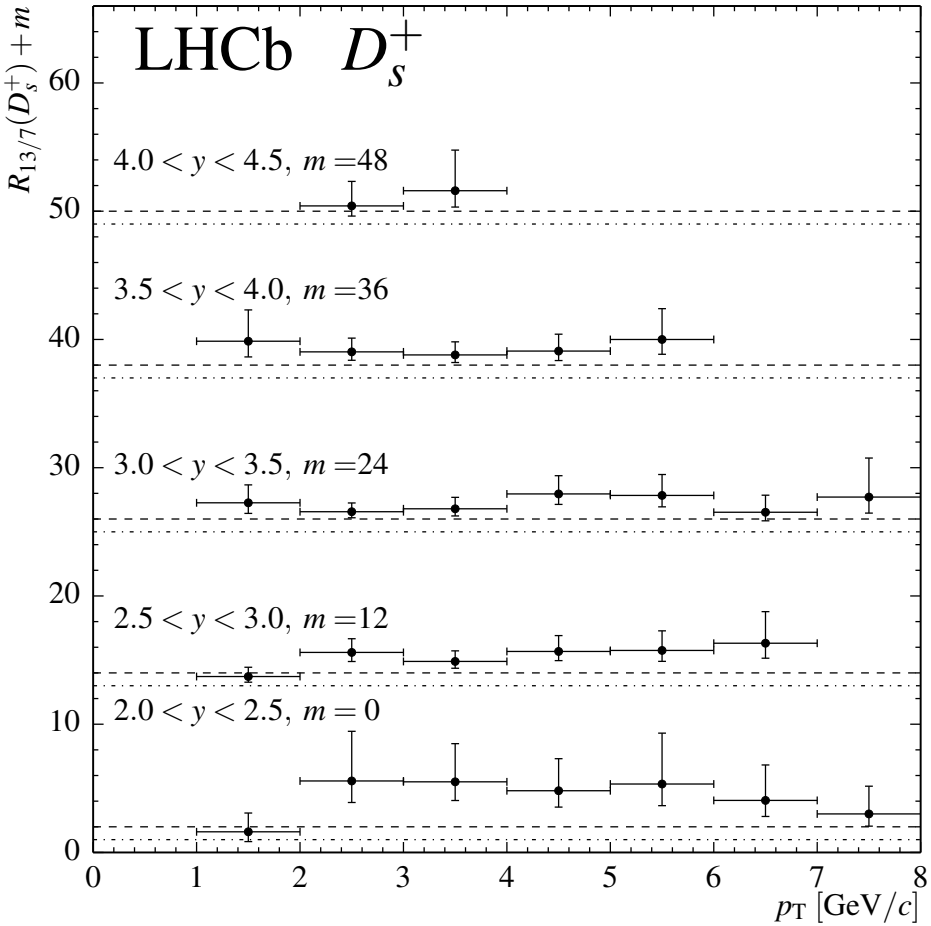

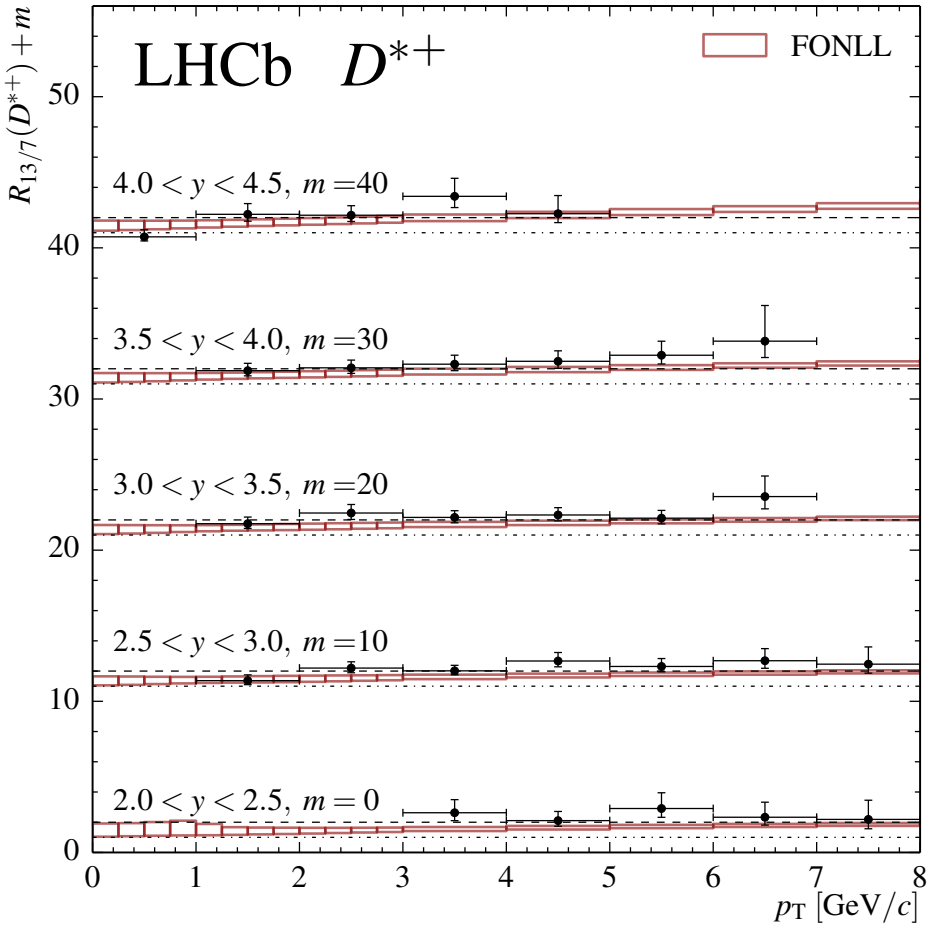

Ratios of double differential cross-sections, $\mathrm{d}^2\sigma_i/\mathrm{d}p_T\mathrm{d}y$, between measurements at $\sqrt{s} = 13\,\mathrm{TeV}$ and at $\sqrt{s} = 7\,\mathrm{TeV}$ (NPB 871 (2013) 1-20).

For each interval, the dash-dotted line represents a ratio of 1.

RATIOS AT 13 TeV: D^+/D^0

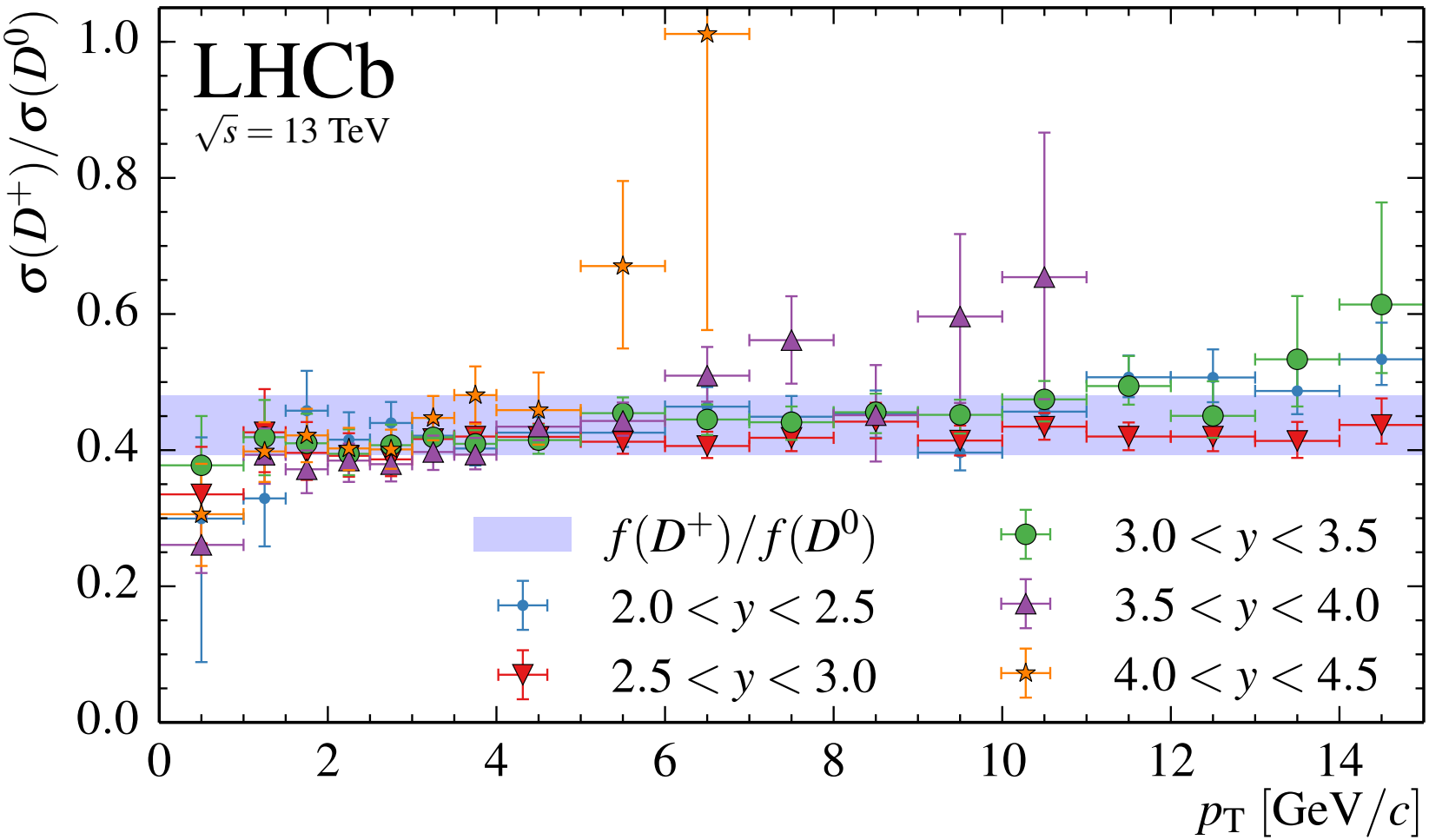

Ratios of double differential cross-sections, $\mathrm{d}^2\sigma_i/\mathrm{d}p_T\mathrm{d}y$, between D^+ and D^0 measurements at $\sqrt{s} = 13$ TeV.

The blue band indicates the ratio of fragmentation fractions from e^+e^-.

RATIOS AT 13 TeV: D_s^+/D^0

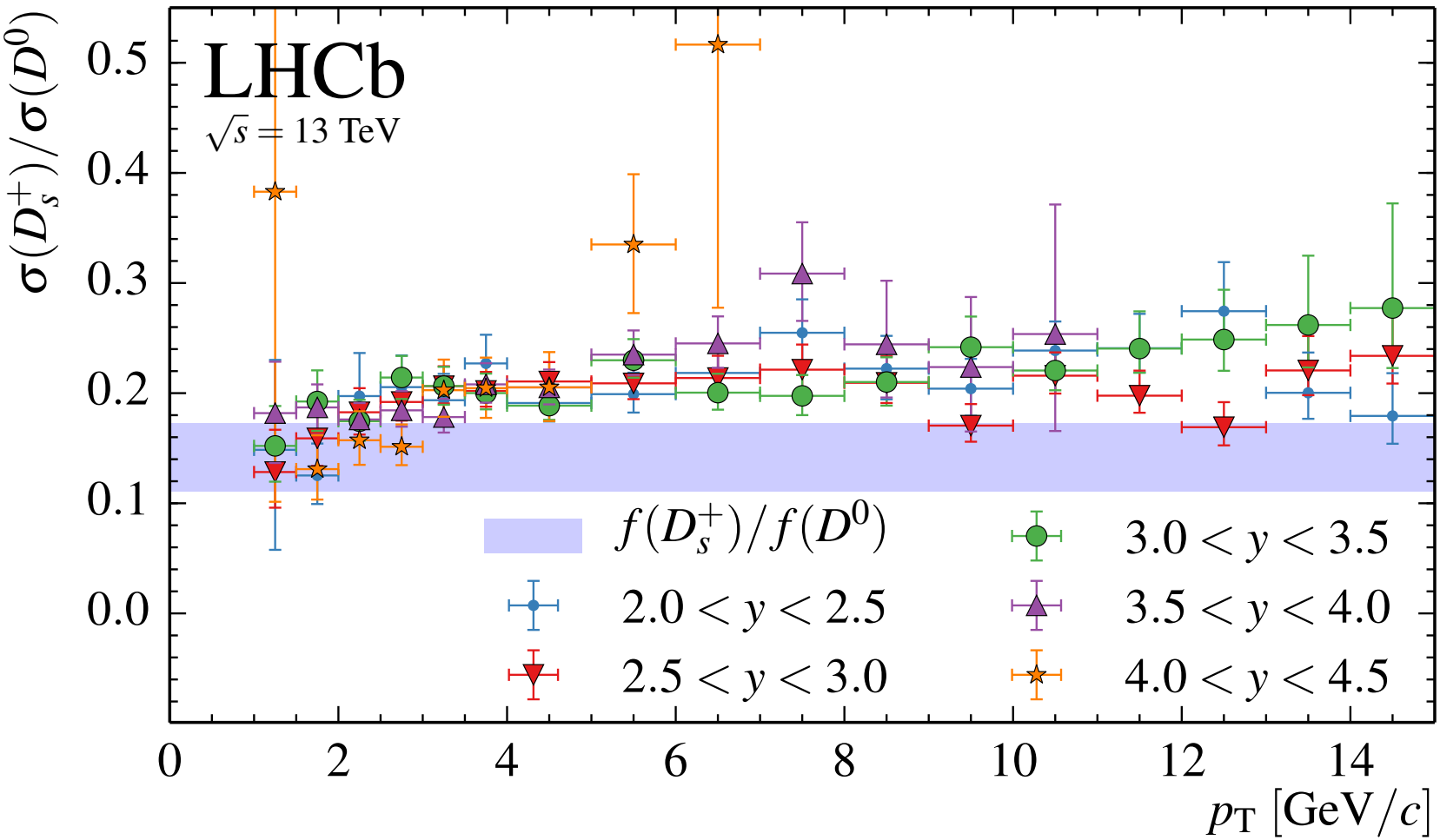

Ratios of double differential cross-sections, $\mathrm{d}^2\sigma_i/\mathrm{d}p_T\mathrm{d}y$, between D_s^+ and D^0 measurements at $\sqrt{s} = 13$ TeV.

The blue band indicates the ratio of fragmentation fractions from e^+e^-.

RATIOS AT 13 TeV: D^{*+}/D^0

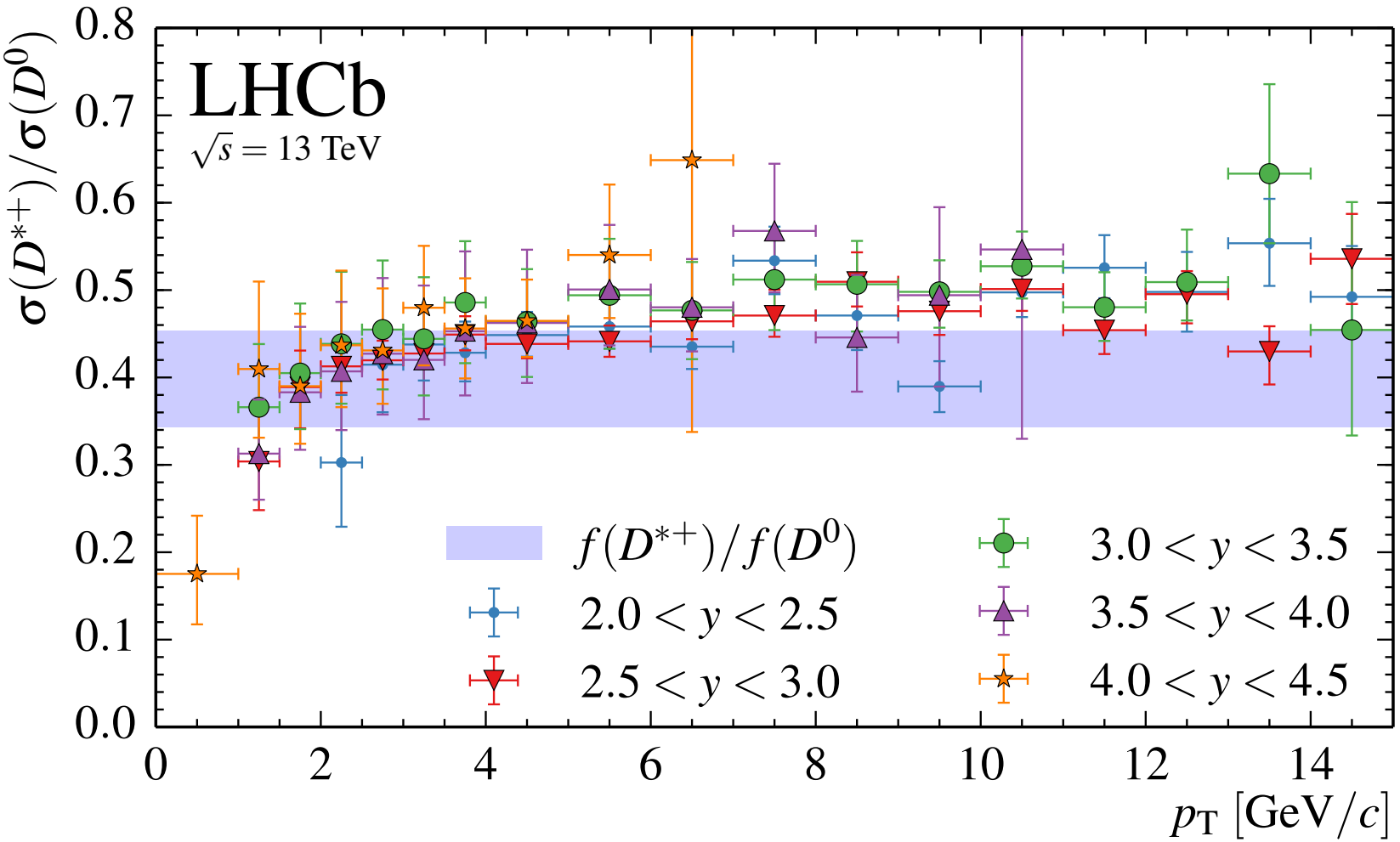

Ratios of double differential cross-sections, $d^2\sigma_i/dp_T dy$, between D^{*+} and D^0 measurements at $\sqrt{s} = 13$ TeV.

The blue band indicates the ratio of fragmentation fractions from e^+e^-.

CONCLUSIONS

LHCb's forward design allows it to probe a unique region of heavy flavor production at LHC.

Proved the efficacy of real-time alignment and calibration of the LHCb detector.

The Turbo stream utilizes the real-time alignment and calibration to provide analysis-ready data directly from the trigger.

- More data and greater physics reach for the computing resources!

The Early Measurements campaign is a great success, with two measurements released and many more in preparation,

- arXiv:1509.00771 (submitted to JHEP): J/ψ and $b\bar{b}$ cross-sections,
- arXiv:1510.01707 (submitted to JHEP): D meson cross-sections.